Technische Universität Berlin
Institut für Mathematik

M002 - Slider Crank[‡] (v1.0)

Andreas Steinbrecher

Preprint 2016/27

Preprint-Reihe des Instituts für Mathematik
Technische Universität Berlin
http://www.math.tu-berlin.de/preprints

Report 2016/27 **December 2016**

The considerations in this report *Slider Crank* are part of the example collection which can be found in `http://www3.math.tu-berlin.de/multiphysics/Examples/`. The aim is to investigate different formulations, i.e., regularized formulations or also index reduced formulations, of the model equations in combination with different numerical solvers with respect to its applicability, efficiency, accuracy, and robustness.

AMS(MOS) subject classification: 65L80

Keywords: example collection, numerical integration, differential-algebraic equations

Authors address:

Institut für Mathematik
Sekretariat MA 4-5
Technische Universität Berlin
Str. d. 17. Juni 136
10623 Berlin
Germany
`anst@math.tu-berlin.de`

Slider Crank

Andreas Steinbrecher

December 15, 2016

Abstract

The considerations in this report *Slider Crank* are part of the example collection which can be found in `http://www3.math.tu-berlin.de/multiphysics/Examples/`. The aim is to investigate different formulations, i.e., regularized formulations or also index reduced formulations, of the model equations in combination with different numerical solvers with respect to its applicability, efficiency, accuracy, and robustness.

Keywords: example collection, numerical integration, differential-algebraic equations

AMS(MOS) subject classification: 65L80

1 Introduction

The considerations in this report *Slider Crank* are part of the example collection which can be found in `http://www3.math.tu-berlin.de/multiphysics/Examples/`. The aim is to investigate different formulations, i.e., regularized formulations or also index reduced formulations, of the model equations in combination with different numerical solvers with respect to its applicability, efficiency, accuracy, and robustness.

2 Slider Crank

In this example we consider the movement of a slider crank with rigid bodies. The simplified topology is illustrated in Figure 1.

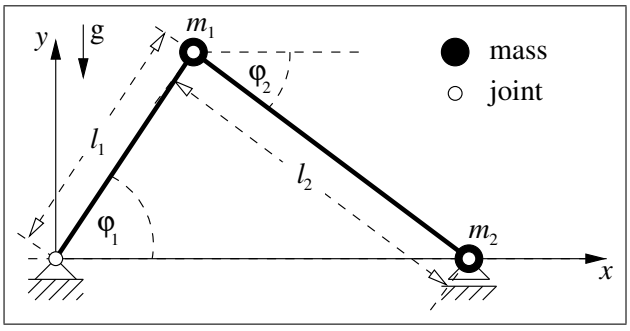

Figure 1: Topology

2.1 Model equations

2.1.1 The Mathematical Model

The mathematical model corresponds to a semi-implicit DAE of strangeness index (s-index) $\nu_s = 2$, of differentiation index (d-index) $\nu_d = 3$, and of maximal constraint level (c-level) $\nu_c = 2$ consisting of 5

‡This work has been supported by European Research Council through Advanced Grant "Modeling, Simulation and Control of Multi-Physics Systems" (MODSIMCONMP)

*Institut für Mathematik, Sekretariat MA 4-5, Technische Universität Berlin, Str. d. 17. Juni 136, 10623 Berlin, Germany, `anst@math.tu-berlin.de`

unknowns, 5 equations, comprising 4 differential equations and 1 algebraic equation. For details on the strangeness-index see [6], the differentiation index see [1, 5], and the maximal constraint level see [7]. The model equations for the slider crank have the form

$$\begin{aligned} \dot{p} &= v, && \text{(1a)} \\ M\dot{v} &= f(p,v) - G^T(p)\lambda, && \text{(1b)} \\ 0 &= g(p) && \text{(1c)} \end{aligned}$$

with $p^T = \begin{bmatrix} p_1 & p_2 \end{bmatrix}$, $v^T = \begin{bmatrix} v_1 & v_2 \end{bmatrix}$, and

$$\begin{aligned} M(p) &= \begin{bmatrix} (m_1+m_2)l_1^2 & -m_2 l_1 l_2 \cos(p_1+p_2) \\ -m_2 l_1 l_2 \cos(p_1+p_2) & m_2 l_2^2 \end{bmatrix}, \\ f(p) &= \begin{bmatrix} -(m_1+m_2)\mathfrak{g} l_1 \cos(p_1) - m_2 l_1 l_2 v_2^2 \sin(p_1+p_2) \\ m_2 \mathfrak{g} l_2 \cos(p_2) - m_2 l_1 l_2 v_1^2 \sin(p_1+p_2) \end{bmatrix}, \\ G(p) = \frac{\partial g}{\partial p}(p) &= \begin{bmatrix} l_1 \cos(p_1) & -l_2 \cos(p_2) \end{bmatrix}, \\ g(p) &= \begin{bmatrix} l_1 \sin(p_1) - l_2 \sin(p_2) \end{bmatrix}, \end{aligned}$$

for $t \in \mathbb{I}$ with the time domain $\mathbb{I} = [t_0, t_f]$. The unknown variables as well as the model parameters are listed in Tables 1 and 2, respectively.

variable	physical meaning	unit	dimension
p_1, p_2	angle between rod 1 and rod 2 and horizon		1 each
v_1, v_2	angular velocity of rod 1 and rod 2	1/s	1 each
λ	Lagrange-Multiplier	kg m/s^2	1

Table 1: Unknown variables

parameter	physical meaning	unit	dimension
m_1, m_2	mass of the mass point 1 and mass point 2	kg	1
l_1, l_2	length of rod 1 and rod 2	m	1
$\mathfrak{g}$	gravitational acceleration	m/s^2	1

Table 2: Parameters

2.1.2 The Origin of the Problem

A slider crank is a mechanism to convert circular motion into rotationally motion, or vice versa. One arm l_1 rotational attached to a shaft is connected by a pivot of mass m_1 with a rod l_2 at one end while the other end of the rod l_2 is attached to a mass m_2. The motion is under gravity $\mathfrak{g}$. Let us use angular coordinates $p_1 = \varphi_1$ and $p_2 = \varphi_2$ denoting the the absolute angle of rod l_1 and the negative absolute angle of rod l_2, respectively.
In the following, (x_i, y_i), $i = 1, 2$ denote the position of mass m_i in Cartesian coordinates and $(v_i, w_i) = (\dot{x}_i, \dot{v}_i)$, $i = 1, 2$ denote the corresponding velocities of mass m_i in x- and y-direction. It holds

$$\begin{bmatrix} x_1 \\ y_1 \end{bmatrix} = l_1 \begin{bmatrix} \cos(p_1) \\ \sin(p_1) \end{bmatrix} \quad \text{and} \quad \begin{bmatrix} x_2 \\ y_2 \end{bmatrix} = l_1 \begin{bmatrix} \cos(p_1) \\ \sin(p_1) \end{bmatrix} + l_2 \begin{bmatrix} \cos(-p_2) \\ \sin(-p_2) \end{bmatrix}.$$

The translational motion of the mass m_2 is constrained to move in a linear sliding motion, here along the x-axis, i.e., $y_2 = 0$ which yields in the constraint

$$0 = g(p) \quad = \quad l_1 \sin(p_1) - l_2 \sin(p_2).$$

Following the Lagrange principle, i.e., Lagrange equation first kind, we obtain for the velocity of mass

m_1

$$\begin{aligned}
||\mathbf{v}_1||_2^2 &= ||\begin{bmatrix} v_1 \\ w_1 \end{bmatrix}||_2^2 = v_1^2 + w_1^2 = \dot{x}_1^2 + \dot{y}_1^2 \\
&= (\frac{\mathrm{d}}{\mathrm{d}t}(l_1\cos(p_1)))^2 + (\frac{\mathrm{d}}{\mathrm{d}t}(l_1\sin(p_1)))^2 \\
&= (-l_1\sin(p_1)\dot{p}_1)^2 + (l_1\cos(p_1)\dot{p}_1)^2 \\
&= l_1^2\sin(p_1)^2\dot{p}_1^2 + l_1^2\cos(p_1)^2\dot{p}_1^2 \\
&= l_1^2(\sin(p_1)^2 + \cos(p_1)^2)\dot{p}_1^2 \\
&= l_1^2\dot{p}_1^2.
\end{aligned}$$

Furthermore, we obtain for the velocity of mass m_2

$$\begin{aligned}
||\mathbf{v}_2||_2^2 &= ||\begin{bmatrix} v_2 \\ w_2 \end{bmatrix}||_2^2 = v_2^2 + w_2^2 = \dot{x}_2^2 + \dot{y}_2^2 \\
&= (\frac{\mathrm{d}}{\mathrm{d}t}(l_1\cos(p_1) + l_2\cos(p_2)))^2 + (\frac{\mathrm{d}}{\mathrm{d}t}(l_1\sin(p_1) - l_2\sin(p_2)))^2 \\
&= (-l_1\sin(p_1)\dot{p}_1 - l_2\sin(p_2)\dot{p}_2)^2 + (l_1\cos(p_1)\dot{p}_1 - l_2\cos(p_2)\dot{p}_2)^2 \\
&= l_1^2\dot{p}_1^2 + l_2^2\dot{p}_2^2 + 2l_1l_2(\sin(p_1)\sin(p_2) - \cos(p_1)\cos(p_2))\dot{p}_1\dot{p}_2 \\
&= l_1^2\dot{p}_1^2 + l_2^2\dot{p}_2^2 - 2l_1l_2\cos(p_1+p_2)\dot{p}_1\dot{p}_2.
\end{aligned}$$

With these velocities we get the kinetic energy T and the potential energy U for the whole system as

$$\begin{aligned}
T &= \frac{1}{2}m_1||\mathbf{v}_1||_2^2 + \frac{1}{2}m_2||\mathbf{v}_2||_2^2 \\
&= \frac{1}{2}m_1l_1^2\dot{p}_1^2 + \frac{1}{2}m_2\big(l_1^2\dot{p}_1^2 + l_2^2\dot{p}_2^2 - 2l_1l_2\cos(p_1+p_2)\dot{p}_1\dot{p}_2\big) \\
&= \frac{1}{2}(m_1+m_2)l_1^2\dot{p}_1^2 + \frac{1}{2}m_2l_2^2\dot{p}_2^2 - m_2l_1l_2\cos(p_1+p_2)\dot{p}_1\dot{p}_2,
\end{aligned}$$

$$\begin{aligned}
U &= m_1\mathfrak{g}y_1 + m_2\mathfrak{g}y_2 \\
&= m_1\mathfrak{g}l_1\sin(p_1) + m_2\mathfrak{g}(l_1\sin(p_1) - l_2\sin(p_2)) \\
&= (m_1+m_2)\mathfrak{g}l_1\sin(p_1) - m_2\mathfrak{g}l_2\sin(p_2).
\end{aligned}$$

The Lagrange function L follows as

$$\begin{aligned}
L &= T - U - g(p)\lambda \\
&= \frac{1}{2}(m_1+m_2)l_1^2\dot{p}_1^2 + \frac{1}{2}m_2l_2^2\dot{p}_2^2 - m_2l_1l_2\cos(p_1+p_2)\dot{p}_1\dot{p}_2 \\
&\quad -((m_1+m_2)\mathfrak{g}l_1\sin(p_1) - m_2\mathfrak{g}l_2\sin(p_2)) \\
&\quad -(l_1\sin(p_1) - l_2\sin(p_2))\lambda \\
&= \frac{1}{2}(m_1+m_2)l_1^2\dot{p}_1^2 + \frac{1}{2}m_2l_2^2\dot{p}_2^2 - m_2l_1l_2\cos(p_1+p_2)\dot{p}_1\dot{p}_2 \\
&\quad -(m_1+m_2)\mathfrak{g}l_1\sin(p_1) + m_2\mathfrak{g}l_2\sin(p_2) \\
&\quad -(l_1\sin(p_1) - l_2\sin(p_2))\lambda.
\end{aligned}$$

For the Lagrange equations

$$0 = \frac{\mathrm{d}}{\mathrm{d}t}(\frac{\partial L}{\partial \dot{\mathbf{p}}}) - \frac{\partial L}{\partial \mathbf{p}}$$

with $\mathbf{p}^T = \left[\begin{array}{ccc} p_1 & p_2 & \lambda \end{array}\right]$ we get w.r.t. p_1

$$\begin{aligned}
&\frac{\mathrm{d}}{\mathrm{d}t}\left(\frac{\partial L}{\partial \dot{p}_1}\right) - \frac{\partial L}{\partial p_1} \\
&= \frac{\mathrm{d}}{\mathrm{d}t}\Big((m_1+m_2)l_1^2\dot{p}_1 - m_2 l_1 l_2 \cos(p_1+p_2)\dot{p}_2\Big) \\
&\quad -\Big(m_2 l_1 l_2 \sin(p_1+p_2)\dot{p}_1\dot{p}_2 - (m_1+m_2)\mathfrak{g} l_1 \cos(p_1) - l_1\cos(p_1)\lambda\Big) \\
&= (m_1+m_2)l_1^2\ddot{p}_1 + m_2 l_1 l_2 \sin(p_1+p_2)(\dot{p}_1+\dot{p}_2)\dot{p}_2 - m_2 l_1 l_2 \cos(p_1+p_2)\ddot{p}_2 \\
&\quad -m_2 l_1 l_2 \sin(p_1+p_2)\dot{p}_1\dot{p}_2 + (m_1+m_2)\mathfrak{g} l_1 \cos(p_1) + l_1\cos(p_1)\lambda \\
&= (m_1+m_2)l_1^2\ddot{p}_1 - m_2 l_1 l_2 \cos(p_1+p_2)\ddot{p}_2 + m_2 l_1 l_2 \sin(p_1+p_2)\dot{p}_2^2 \\
&\quad +(m_1+m_2)\mathfrak{g} l_1 \cos(p_1) + l_1\cos(p_1)\lambda.
\end{aligned}$$

Therefore, we get the dynamical equation of motion for p_1 as

$$\begin{aligned}
\left[\begin{array}{cc} (m_1+m_2)l_1^2 & -m_2 l_1 l_2 \cos(p_1+p_2) \end{array}\right] \left[\begin{array}{c} \ddot{p}_1 \\ \ddot{p}_2 \end{array}\right] &= \left[\begin{array}{c} -m_2 l_1 l_2 \sin(p_1+p_2)\dot{p}_2^2 - (m_1+m_2)\mathfrak{g} l_1 \cos(p_1) \end{array}\right] \\
&\quad - \left[\begin{array}{c} l_1 \cos(p_1) \end{array}\right]\lambda. \qquad (2)
\end{aligned}$$

Furthermore, from the Lagrange equations we get w.r.t. p_2

$$\begin{aligned}
&\frac{\mathrm{d}}{\mathrm{d}t}\left(\frac{\partial L}{\partial \dot{p}_2}\right) - \frac{\partial L}{\partial p_2} \\
&= \frac{\mathrm{d}}{\mathrm{d}t}(m_2 l_2^2\dot{p}_2 - m_2 l_1 l_2 \cos(p_1+p_2)\dot{p}_1) \\
&\quad -(m_2 l_1 l_2 \sin(p_1+p_2)\dot{p}_1\dot{p}_2 + m_2\mathfrak{g} l_2 \cos(p_2) l_2 \cos(p_2)\lambda) \\
&= m_2 l_2^2\ddot{p}_2 + m_2 l_1 l_2 \sin(p_1+p_2)(\dot{p}_1+\dot{p}_2)\dot{p}_1 - m_2 l_1 l_2 \cos(p_1+p_2)\ddot{p}_1 \\
&\quad -m_2 l_1 l_2 \sin(p_1+p_2)\dot{p}_1\dot{p}_2 - m_2\mathfrak{g} l_2 \cos(p_2) - l_2\cos(p_2)\lambda \\
&= m_2 l_2^2\ddot{p}_2 - m_2 l_1 l_2 \cos(p_1+p_2)\ddot{p}_1 + m_2 l_1 l_2 \sin(p_1+p_2)\dot{p}_1^2 - m_2\mathfrak{g} l_2 \cos(p_2) - l_2\cos(p_2)\lambda.
\end{aligned}$$

Therefore, we get the dynamical equation of motion for p_2 as

$$\begin{aligned}
\left[\begin{array}{cc} -m_2 l_1 l_2 \cos(p_1+p_2) & m_2 l_2^2 \end{array}\right] \left[\begin{array}{c} \ddot{p}_1 \\ \ddot{p}_2 \end{array}\right] &= \left[\begin{array}{c} -m_2 l_1 l_2 \sin(p_1+p_2)\dot{p}_1^2 + m_2\mathfrak{g} l_2 \cos(p_2) \end{array}\right] \\
&\quad - \left[\begin{array}{c} -l_2 \cos(p_2) \end{array}\right]\lambda. \qquad (3)
\end{aligned}$$

Furthermore, from the Lagrange equations we get w.r.t. λ

$$\frac{\mathrm{d}}{\mathrm{d}t}\left(\frac{\partial L}{\partial \dot{\lambda}}\right) - \frac{\partial L}{\partial \lambda} = l_1 \sin(p_1) - l_2 \sin(p_2).$$

Therefore, we get the dynamical equation of motion for λ as the constraint

$$0 = l_1 \sin(p_1) - l_2 \sin(p_2). \qquad (4)$$

Summarizing (2)-(4) we get the equations of motion in second order form as

$$\begin{aligned}
&\left[\begin{array}{cc} (m_1+m_2)l_1^2 & -m_2 l_1 l_2 \cos(p_1+p_2) \\ -m_2 l_1 l_2 \cos(p_1+p_2) & m_2 l_2^2 \end{array}\right] \left[\begin{array}{c} \ddot{p}_1 \\ \ddot{p}_2 \end{array}\right] \\
&\qquad = \left[\begin{array}{c} -m_2 l_1 l_2 \sin(p_1+p_2)\dot{p}_2^2 - (m_1+m_2)\mathfrak{g} l_1 \cos(p_1) \\ -m_2 l_1 l_2 \sin(p_1+p_2)\dot{p}_1^2 + m_2\mathfrak{g} l_2 \cos(p_2) \end{array}\right] - \left[\begin{array}{c} l_1\cos(p_1) \\ -l_2\cos(p_2) \end{array}\right]\lambda, \\
&\qquad 0 = l_1 \sin(p_1) - l_2 \sin(p_2).
\end{aligned}$$

Reformulation and introduction of $v = \dot{p}$ yields (1).
Since the slider crank is only influenced by the gravitational field of forces, i.e., by a conservative field of forces, and since it is not affected by other applied forces, it represents a mechanical system which conserves the total energy. This total energy is given by

$$\begin{aligned}
E(p,v) = T + U &= \Big(\frac{1}{2}(m_1+m_2)l_1^2 v_1^2 + \frac{1}{2}m_2 l_2^2 v_2^2 - m_2 l_1 l_2 \cos(p_1+p_2)v_1 v_2\Big) \\
&\quad +\Big((m_1+m_2)\mathfrak{g} l_1 \sin(p_1) - m_2\mathfrak{g} l_2 \sin(p_2)\Big)
\end{aligned}$$

and is conserved such that we get the *constraint of energy conservation*

$$\begin{aligned} 0 = e(x,y,v,w) &= E(x,y,v,w) - E(x_0,y_0,v_0,w_0) \\ &= \Big(\frac{1}{2}(m_1+m_2)l_1^2v_1^2 + \frac{1}{2}m_2l_2^2v_2^2 - m_2l_1l_2\cos(p_1+p_2)v_1v_2\Big) \\ &\quad +\Big((m_1+m_2)\mathfrak{g}l_1\sin(p_1) - m_2\mathfrak{g}l_2\sin(p_2)\Big) \\ &\quad -\Big(\frac{1}{2}(m_1+m_2)l_1^2(v_1^0)^2 + \frac{1}{2}m_2l_2^2(v^0)_2^2 - m_2l_1l_2\cos(p_1^0+p_2^0)v_1^0v_2^0\Big) \\ &\quad -\Big((m_1+m_2)\mathfrak{g}l_1\sin(p_1^0) - m_2\mathfrak{g}l_2\sin(p_2^0)\Big) \end{aligned} \tag{5}$$

which is satisfied for all $t \in \mathbb{I}$ for every solution of the equations of motion (1) with initial values p_i^0, v_i^0, $i = 1, 2$.
The unknown variables as well as the model parameters are listed in Tables 1 and 2, respectively. The values of the parameters, the initial values, and the time domain are specified in detail in the scenarios below.

2.1.3 Analysis of the Model Equations

Hidden Constraints Solutions of the model equations are restricted by so called *hidden constraints* which, in particular, are responsible for the difficulties in the numerical treatment. In particular, as one hidden constraint we have the *holonomic constraint of velocity level*

$$0 = g^I(p,v) := l_1\cos(p_1)v_1 - l_2\cos(p_2)v_2 \tag{6a}$$

obtained from the total time derivative of the holonomic constraints (1c), where the derivatives $\dot{p}_i$ are replaced by (1a). The constraint (6a) is also called *hidden constraint of level 1* since this constraint is obtained after differentiation of (certain) model equations once. A further hidden constraint is the *holonomic constraint of acceleration level*

$$0 = g^{II}(p,v,\lambda) := -l_1\sin(p_1)v_1^2 + l_1\cos(p_1)a_1 + l_2\sin(p_2)v_2^2 - l_2\cos(p_2)a_2, \tag{6b}$$

where a_1 and a_2 correspond to the angular acceleration of the rods and are determined from (1b) as

$$\begin{bmatrix} a_1 \\ a_2 \end{bmatrix} = (M(p))^{-1}\begin{bmatrix} -(m_1+m_2)\mathfrak{g}l_1\cos(p_1) - m_2l_1l_2v_2^2\sin(p_1+p_2) \\ m_2\mathfrak{g}l_2\cos(p_2) - m_2l_1l_2v_1^2\sin(p_1+p_2) \end{bmatrix}.$$

This is obtained from the total time derivative of the holonomic constraint on velocity level (6a), where the derivatives $\dot{p}_i$ and $\dot{v}_i$ are replaced by (1a), (1b), respectively. The constraint (6b) is also called *hidden constraint of level 2* since this constraint is obtained after differentiation of (certain) model equations twice.

2.1.4 Regularizations and used Formulations

For the numerical treatment we will use the following formulations.

d-index 2 formulation (rcd1) The *d-index 2 formulation* has the form

$$\dot{p} = v, \tag{7a}$$
$$M\dot{v} = f(p,v) - G^T(p)\lambda, \tag{7b}$$
$$0 = g^I(p,v) \tag{7c}$$

and belongs to the classical index reduction, where in the model equations (1) the holonomic constraint (1c) is replaced by the holonomic constraint on velocity level (6a). This formulation has d-index 2, s-index 1, and maximal constraint level 1 and contains (6b) as hidden constraint of level 1 while the constraint (1c) is removed. Therefore, in its numerical treatment slight instabilities due to the higher index, i.e., the existence of hidden constraints, and linear drift from the holonomic constraint (1c) is expected due to the loss of this constraint on position level. For more details we refer to [5, 7].

d-index 1 formulation (rcd0) The *d-index 1 formulation* has the form

$$\begin{aligned} \dot{p} &= v, && \text{(8a)} \\ M\dot{v} &= f(p,v) - G^T(p)\lambda, && \text{(8b)} \\ 0 &= g^{II}(p,v) && \text{(8c)} \end{aligned}$$

and belongs to the classical index reduction, where in the model equations (1) the holonomic constraint (1c) is replaced by holonomic constraint on acceleration level (6b). This formulation has d-index 1, s-index 0, and maximal constraint level 0 and contains no hidden constraint while the constraints (1c) and (6a) are removed. Therefore, in its numerical treatment no instabilities but quadratic drift from the holonomic constraint (1c) and linear drift from the holonomic constraint on velocity level (6a) is expected due to the loss of the constraint on position level (1c) and the constraint on velocity level (6a). For more details we refer to [5, 7].

overdetermined c-level 1 formulation (ovd1) The *overdetermined c-level 1 formulation* has the form

$$\begin{aligned} \dot{p} &= v, && \text{(9a)} \\ M\dot{v} &= f(p,v) - G^T(p)\lambda, && \text{(9b)} \\ 0 &= g(p), && \text{(9c)} \\ 0 &= g^{I}(p,v) && \text{(9d)} \end{aligned}$$

where the holonomic constraint on velocity level (6a) is added to the model equations (1). This formulation has s-index 1, and maximal constraint level 1 while the d-index is not defined. Furthermore, this formulation contains (6b) as hidden constraint of level 1 while no constraint is removed. Therefore, in its numerical treatment slight instabilities due to the higher c-level, i.e., the existence of hidden constraints, but no drift are expected. The direct numerical integration needs adapted numerical methods suited for overdetermined DAEs. For more details we refer to [2, 7].

overdetermined c-level 0 formulation (ovd0) The *overdetermined c-level 0 formulation* has the form

$$\begin{aligned} \dot{p} &= v, && \text{(10a)} \\ M\dot{v} &= f(p,v) - G^T(p)\lambda, && \text{(10b)} \\ 0 &= g(p), && \text{(10c)} \\ 0 &= g^{I}(p,v), && \text{(10d)} \\ 0 &= g^{II}(p,v,\lambda) && \text{(10e)} \end{aligned}$$

where the holonomic constraint on velocity level (6a) and the holonomic constraint on acceleration level (6b) are added to the model equations (1). This formulation has s-index 1, and maximal constraint level 0 while the d-index is not defined. Furthermore, this formulation contains no hidden constraint while no constraint is removed. Therefore, in its numerical treatment no instabilities and no drift are expected. The direct numerical integration needs adapted numerical methods suited for overdetermined DAEs. For more details we refer to [2, 7].

2.2 Numerical Results

For the numerical computations we use the following solvers combined with the original model equations (1) (denoted by (ori2)) and the regularized formulations presented in Section 2.1.4.

`DASPK` (Version 2.0 from 12.Jul.2000) [10] is suited for nonlinear DAEs of d-index 1 and uses BDF-methods of order 1 up to 5 as discretization scheme.

`GEOMS` (Version 1.3 from 17.Nov.2014) [7, 8] is suited for equations of motion for multibody systems and its regularizations based on overdetermined formulations and uses the Runge-Kutta method of type RADAU IIa of order 5 as discretization scheme.

`ODASSL` (Version from 03.Jan.1990) [2, 3] is suited for (possibly overdetermined) nonlinear DAEs with maximal c-level 0 and uses an adaption of the BDF-methods of order 1 up to 5 as discretization scheme.

QUALIDAES (Version 0.1 from 09.Sep.2015) [9] is suited for (possibly overdetermined) quasi-linear DAEs with maximal c-level 1 and uses an adaption of the Runge-Kutta method of type RADAU IIa of order 5 as discretization scheme.

Note that RADAU5 [4, 5] cannot be applied to the model equations (1) since RADAU5 requires a constant leading matrix M what is not the case in (1). The numerical integrations are done on an AMD Phenom(tm) II X6 1090T, 3210 MHz.

2.2.1 Scenario 01

The equations of motion are given in (1).

m_1	$= 1$ kg	l_1	$= 1$ m	$\mathfrak{g}$	$= 9.81$ m/s^2
m_2	$= 1.8$ kg	l_1	$= 3$ m		

Table 3: Scenario 01: Parameters

In that scenario we will simulate the motion of the slider crank on $\mathbb{I} = [0\text{s}, 100\text{s}]$ with the parameters as depicted in Table 3 and the initial values

$$\begin{aligned} p_1(t_0) = p_1^0 &= 0, \quad v_1(t_0) = v_1^0 = 0, \quad \lambda(t_0) = \lambda^0 = -17.658\ (= -m_2\mathfrak{g}), \\ p_2(t_0) = p_2^0 &= 0, \quad v_2(t_0) = v_2^0 = 0. \end{aligned} \tag{11}$$

Reference Solution Since this problem is not analytically solvable, we use the numerical solution obtained with GEOMS for the overdetermined c-level 0 formulation (ovd0) with a prescribed tolerance ATOL=RTOL=10^{-14} as reference solution for comparisons of the obtained precision.

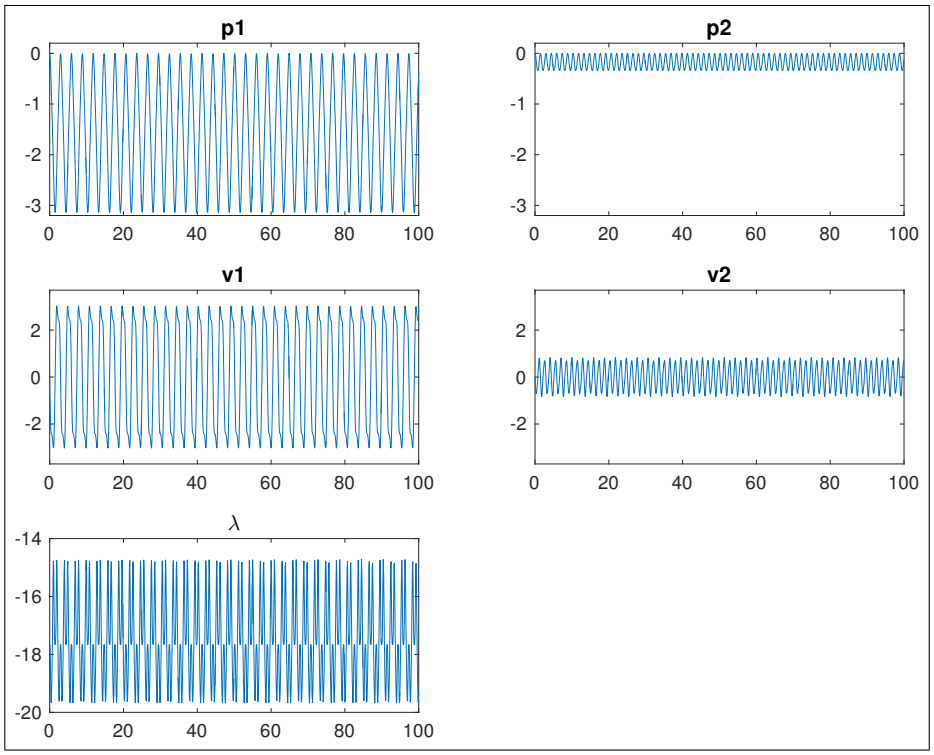

Figure 2: Scenario 01: Reference solution

In Figure 2 the reference solution is illustrated, while in Figure 3 the reference solution for the first 10s is illustrated. Furthermore, in Table 4 the values of the reference solution at the final time $t_f = 100$s are listed.

Numerical Solution For the numerical computations the tolerances RTOL=ATOL=10^{-i}, $i = 5, ..., 12$ are prescribed uniformly for all components of the state variables. Selected driver subroutines for the

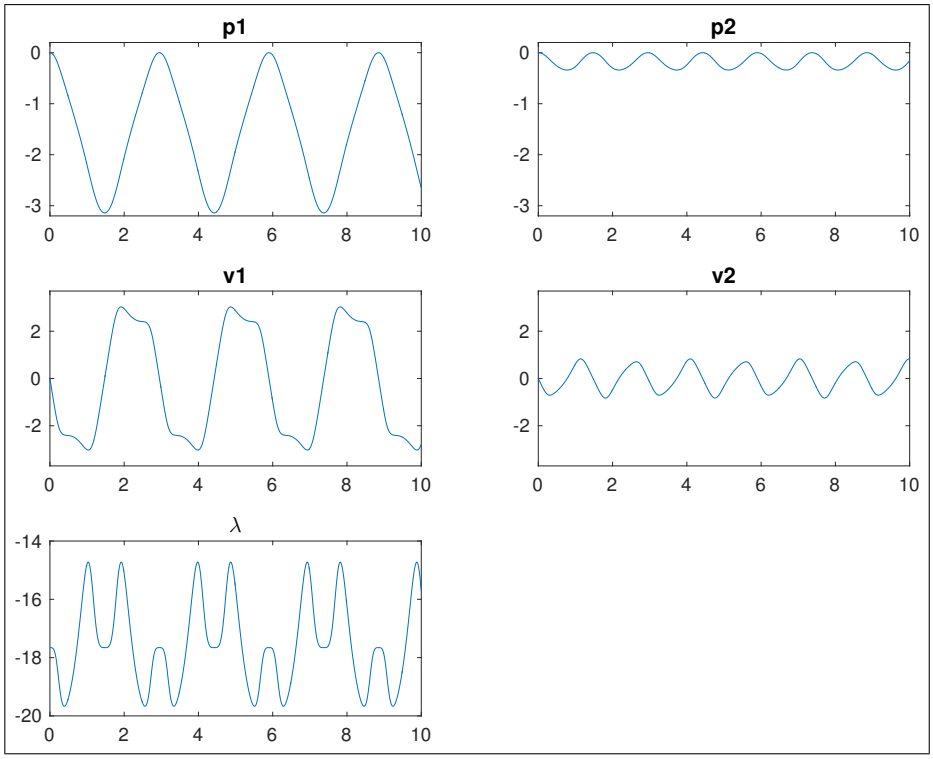

Figure 3: Scenario 01: Reference solution for the first 10s only, i.e., $\mathbb{I} = [0\text{s}, 10\text{s}]$

$x(t_f) =$	-0.3702429132554788D+00	$y(t_f) =$	-0.1209083397446106D+00
$v(t_f) =$	0.2246818213774976D+01	$w(t_f) =$	0.7033255158947435D+00
$\lambda(t_f) =$	-0.1926354617075898D+02		

Table 4: Scenario 01: Reference solution at the final time point $t_f = 100$s.

used solver-formulation combinations are available on the webpage `http://www3.math.tu-berlin.de/multiphysics/Examples/M002_SliderCrank/`. The used solver-formulation combinations and an overview of the success is illustrated in Table 5. Here it can be seen that the numerical integration using the the d-index 2 formulation (rcd1) is only successful with `QUALIDAES` (for some prescribed tolerances) due to its higher index. Furthermore, the numerical integration using the overdetermined c-level 1 formulation (ovd1) was only successful in combination with `QUALIDAES` (for some prescribed tolerances) and `GEOMS` (for some prescribed tolerances) since `GEOMS` internally uses a scaling of the unknown variables due to the special structure of the equations of motion for multibody systems. Neither `ODASSL` nor `QUALIDAES` offers such an automatic scaling. In particular, all numerical integrations based on the d-index 1 formulation (rcd0) and on the overdetermined c-level 0 formulation (ovd0) are successful independent of the used numerical method.

	rcd1	rcd0	ovd1	ovd0
`DASPK`	o[1]	X	-[4]	-[4]
`GEOMS`	-[5]	-[5]	X	X
`ODASSL`	o[1]	X	o[1]	X
`QUALIDAES`	x	X	x	X

'X' successful for every prescribed tolerance
'x' successful for some/few prescribed tolerances
'o' not successful for every prescribed tolerance
'-' formulation does not satisfy the structural requirements of the solver

[1] not suitable for DAEs consisting hidden constraints (c-level>0)
[4] not suitable for overdetermined DAEs
[5] `GEOMS` is only suited for MBS structure including at least hidden constraints on velocity level

Table 5: Scenario 01: Used solver-formulation combinations and an overview of the success

In Figure 4 we have illustrated the solution of the numerical integration for the whole time domain $\mathbb{I}$ for all solver-formulation combinations with a prescribed tolerance `RTOL`=`ATOL`=10^{-6}. In Figure 5

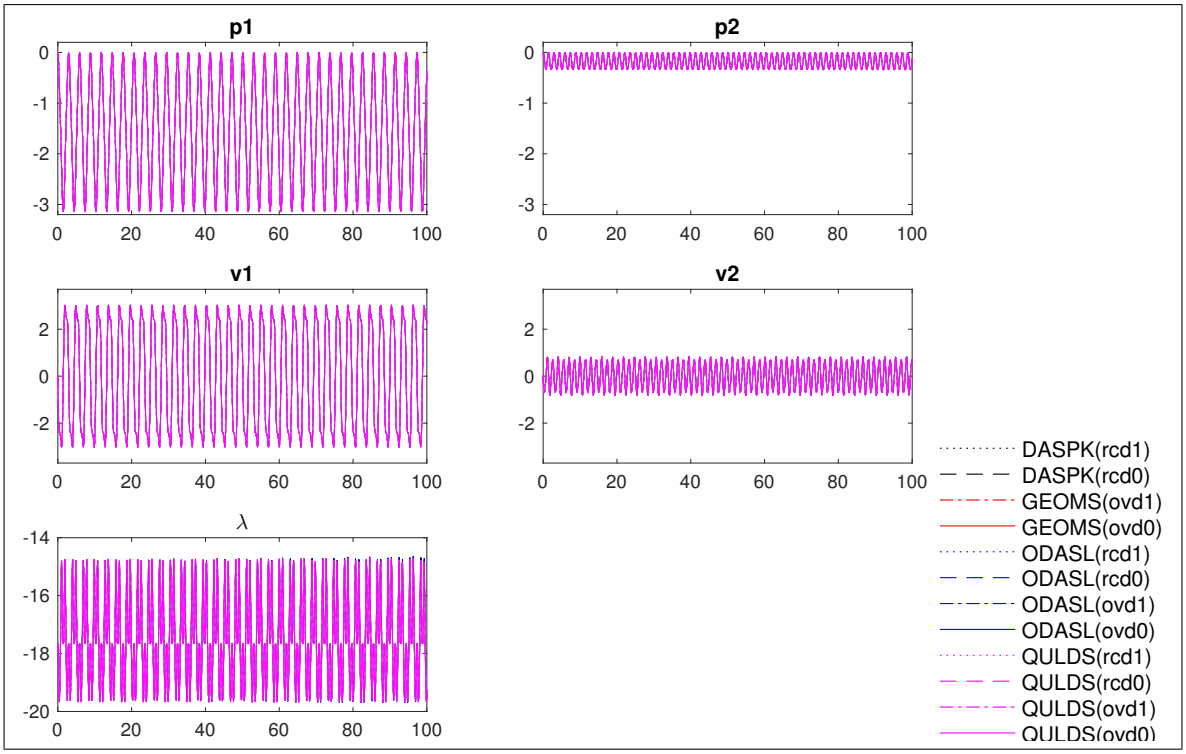

Figure 4: Scenario 01: Numerical solutions for a prescribed tolerance of RTOL=ATOL=10^{-6}

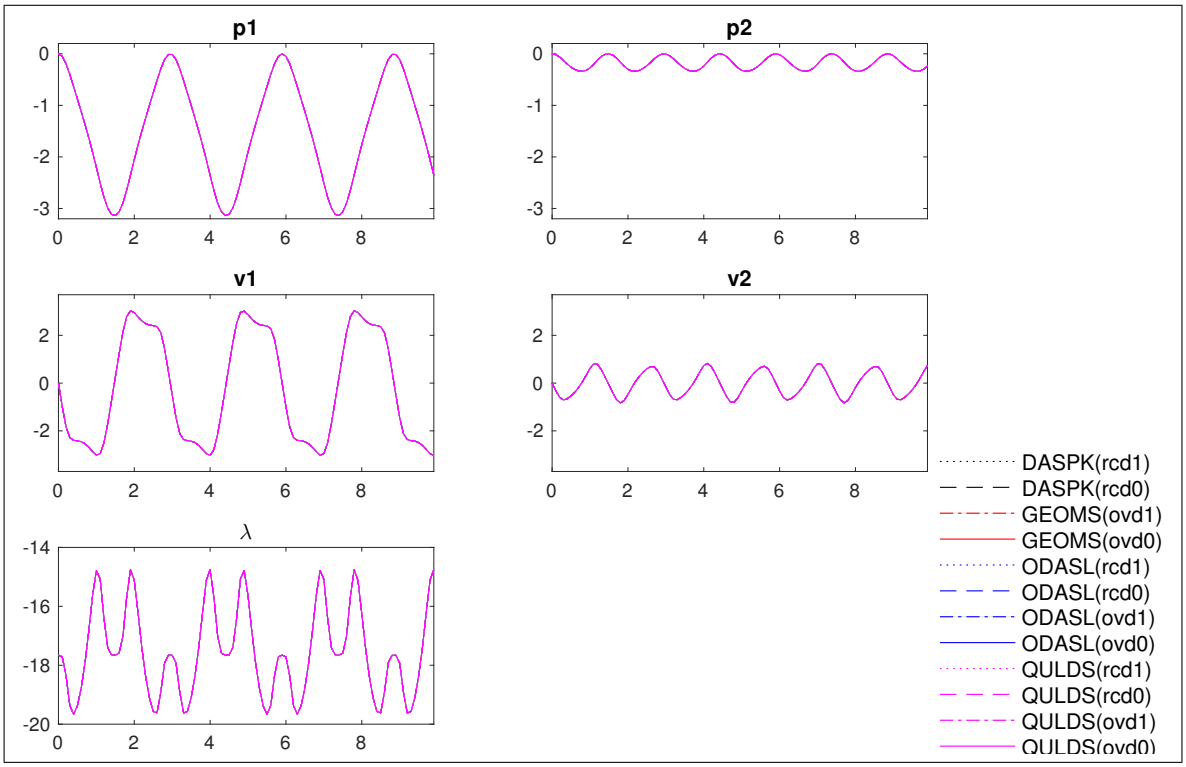

Figure 5: Scenario 01: Numerical solutions (zoom) for a prescribed tolerance of RTOL=ATOL=10^{-6}

these solutions of the numerical integration are illustrated for the time domain $[0\text{s}, 10\text{s}]$. Furthermore, in Figure 6 the obtained error of these numerical solutions is illustrated in logarithmic style. The largest deviation show the solutions ODASSL(rcd0) and DASPK(rcd0) which mainly comes from the drift due to the missing constraints (1c) and (6a) in the d-index 1 formulation (rcd0) (8) which leads up to quadratic

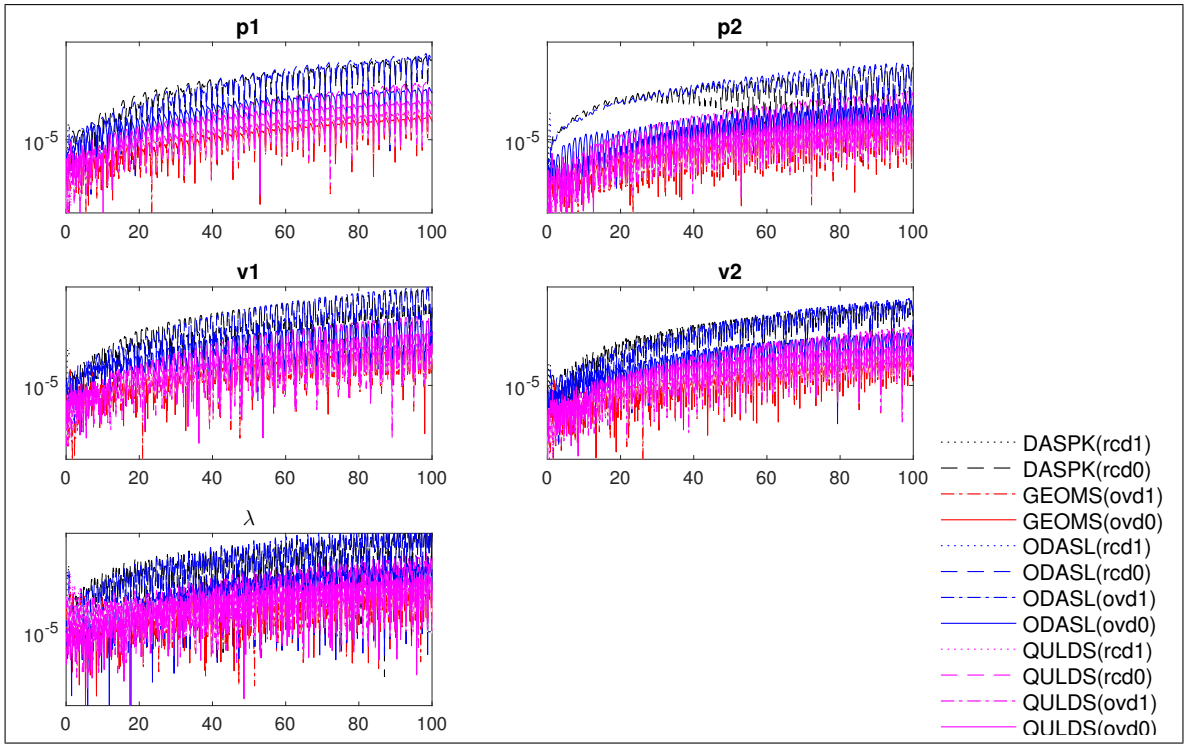

Figure 6: Scenario 01: Numerical error for a prescribed tolerance of RTOL=ATOL=10^{-6}

drift from the constraint of position level (1c) and linear drift from the constraint of velocity level (6a), as illustrated in Figure 7. The best accuracy for the prescribed tolerance is obtained by the usage of the solvers GEOMS(ovd0), GEOMS(ovd1), QUALIDAES(ovd1), and QUALIDAES(ovd0) and also slightly reduced for ODASSL(ovd0).

In Figure 7 we have illustrated the absolute residuals of the constraints, i.e., the constraint (1c), the hidden constraints (6a),(6b), as well as the energy conserving constraint (5) for a selection of the numerical results. The numerical solutions show the behavior depending on the used formulations as expected in the regulatrizations, see Section 2.1.4. So the constraint on position level (1c) is mainly violated with a large deviation from DASPK(rcd0), ODASSL(rcd0), and QUALIDAES(rcd0). Furthermore, the numerical results DASPK(rcd1) and ODASSL(rcd1) show large deviation in the beginning of the time integration. This deviation is caused by the (expected) drift off effect and the higher index of the used formulation (rcd1) and (rcd0). The other violation of the constraints of position level for the other solver-formulation combinations fits into the prescribed tolerance of 10^{-6}.

The constraints on velocity level are significantly violated for DASPK(rcd0) and ODASSL(rcd0) and moderately violated for QUALIDAES(rcd0). The other violation of the constraints of position level for the other solver-formulation combinations fits into the prescribed tolerance of 10^{-6}.

The constraint on acceleration level only for the usage of (rcd1) is violated significantly (in the beginning of $\mathbb{I}$) due to its c-level 1 and the existence of the constraint on acceleration as hidden constraints.

The energy conservation is obtained very good for the numerical results obtained with GEOMS(ovd0), GEOMS(ovd1), and for the solver-formulation combination QUALIDAES(ovd1) and QUALIDAES(ovd0). Furthermore, the numerical results ODASSL(ovd0) conserve the energy acceptable, while the numerical results obtained for the formulations (rcd0) and (rcd1) do not show any energy conservation due to the drift of effect for (rcd0) and (rcd1).

Details in the efficiency for all computations with at least one successful run are listed in Table 6 and illustrated in Figure 8. In particular, ODASSL with the formulations (rcd0) and (ovd0) offers the best efficiency for this scenario. In particular, this is very good for the usage of the index-reduced formulation (rcd0), where the constraints on position level and on velocity level are lost such that the solution drifts away from the position as well as velocity level constraints. Furthermore, a very good performance is offered from QUALIDAES(rcd0), QUALIDAES(ovd0), GEOMS(ovd0), and DASPK(rcd0) while GEOMS(ovd1) offers a reduced performance. Nevertheless, GEOMS and QUALIDAES are the only solvers which are able to integrate a formulation (here (ovd1)) still containing hidden constraints. The maximally obtained precisions are comparable for all successful integrations. For quantitative details in the efficiency, see

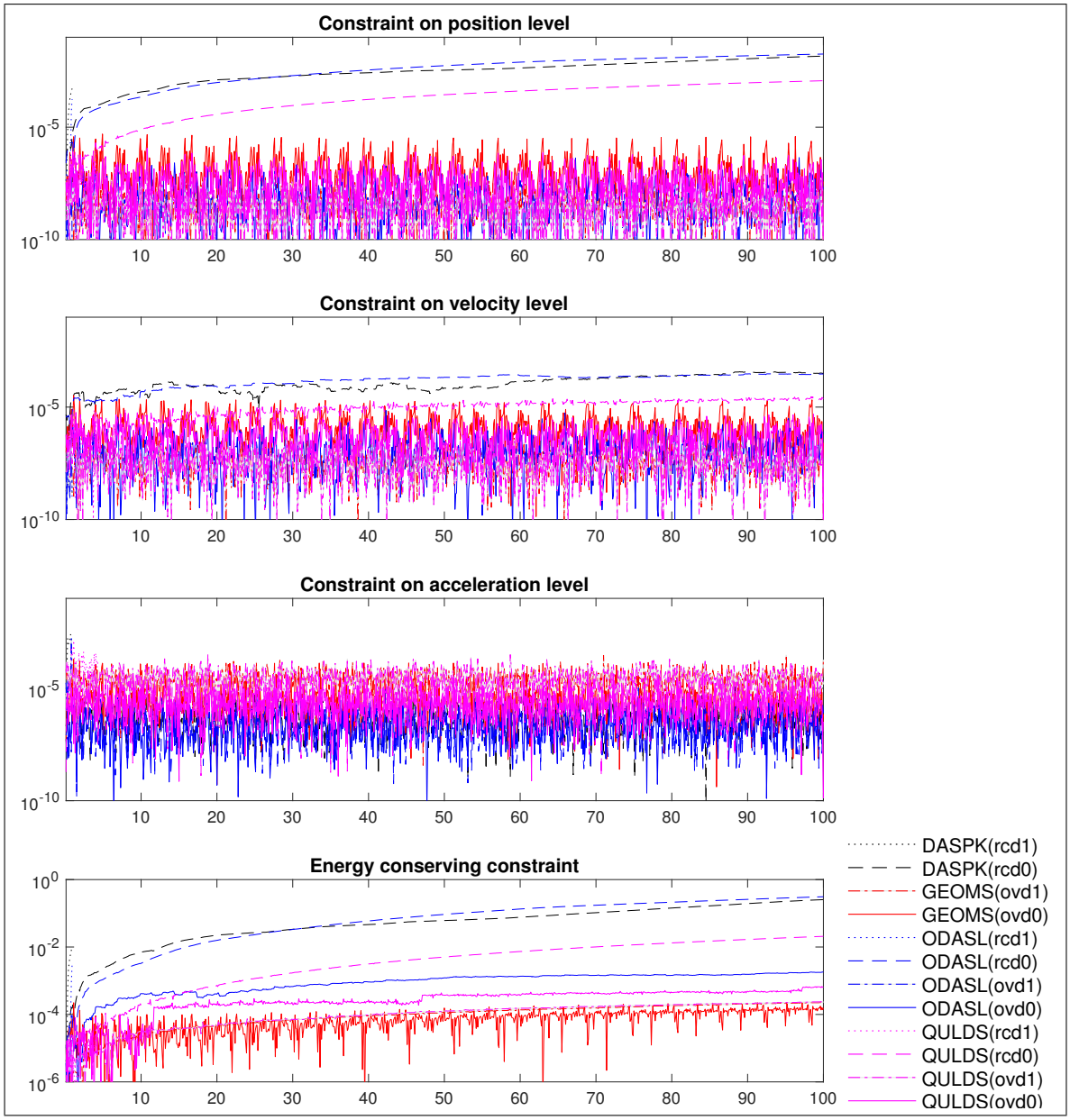

Figure 7: Scenario 01: Residuum of the constraints for a prescribed tolerance of RTOL=ATOL=10^{-6}

Table 6.

	Tol	10^{-5}	10^{-6}	10^{-7}	10^{-8}	10^{-9}	10^{-10}	10^{-11}	10^{-12}
DASPK(rcd0)	Tsim	3.2e-02	4.0e-02	4.8e-02	6.8e-02	9.6e-02	1.3e-01	1.8e-01	2.4e-01
	ERR	1.3e+00	3.7e-01	4.4e-03	2.7e-03	6.6e-04	2.6e-04	6.5e-05	6.0e-06
GEOMS(ovd1)	Tsim	1.1e-01	1.5e-01	2.1e-01	3.2e-01	5.0e-01	7.9e-01	1.3e+00	2.0e+00
	ERR	2.5e-02	2.4e-03	2.5e-04	4.3e-05	9.0e-06	2.1e-06	4.2e-07	9.5e-08
GEOMS(ovd0)	Tsim	8.8e-02	1.1e-01	1.2e-01	1.6e-01	2.1e-01	2.8e-01	4.0e-01	5.6e-01
	ERR	1.1e-02	1.5e-03	4.2e-04	5.5e-05	1.6e-05	3.0e-06	4.9e-07	9.3e-08
ODASSL(rcd0)	Tsim	2.8e-02	4.0e-02	4.8e-02	6.4e-02	8.4e-02	1.2e-01	1.7e-01	2.6e-01
	ERR	3.9e+00	5.0e-01	4.5e-03	3.5e-03	1.6e-03	2.7e-05	2.7e-06	4.1e-06
ODASSL(ovd0)	Tsim	3.6e-02	4.8e-02	6.4e-02	8.8e-02	1.2e-01	1.7e-01	2.4e-01	3.6e-01
	ERR	1.3e-01	2.1e-02	3.9e-03	3.1e-04	3.4e-05	4.2e-06	4.7e-07	1.8e-07
QUALIDAES(rcd1)	Tsim	-	-	-	-	-	-	8.3e-01	8.0e-03
	ERR	-	-	-	-	-	-	4.5e-07	-
QUALIDAES(rcd0)	Tsim	4.4e-02	5.2e-02	7.2e-02	9.6e-02	1.3e-01	1.8e-01	2.6e-01	3.6e-01
	ERR	2.1e-01	3.2e-02	8.1e-03	3.9e-04	1.2e-04	4.0e-05	9.0e-06	1.3e-06
QUALIDAES(ovd1)	Tsim	7.2e-02	9.2e-02	1.4e-01	2.2e-01	3.4e-01	5.5e-01	8.7e-01	-
	ERR	2.5e-02	2.7e-03	3.1e-04	5.0e-05	9.7e-06	2.0e-06	4.3e-07	-
QUALIDAES(ovd0)	Tsim	6.0e-02	7.6e-02	1.0e-01	1.3e-01	1.7e-01	2.4e-01	3.2e-01	4.5e-01
	ERR	2.6e-01	6.3e-03	3.8e-03	2.8e-05	6.4e-05	1.0e-04	4.0e-07	1.1e-06

Tsim - Simulation time in seconds, ERR - error w.r.t. reference solution, '-' numerical integration was not successful

Table 6: Scenario 01: Efficiency

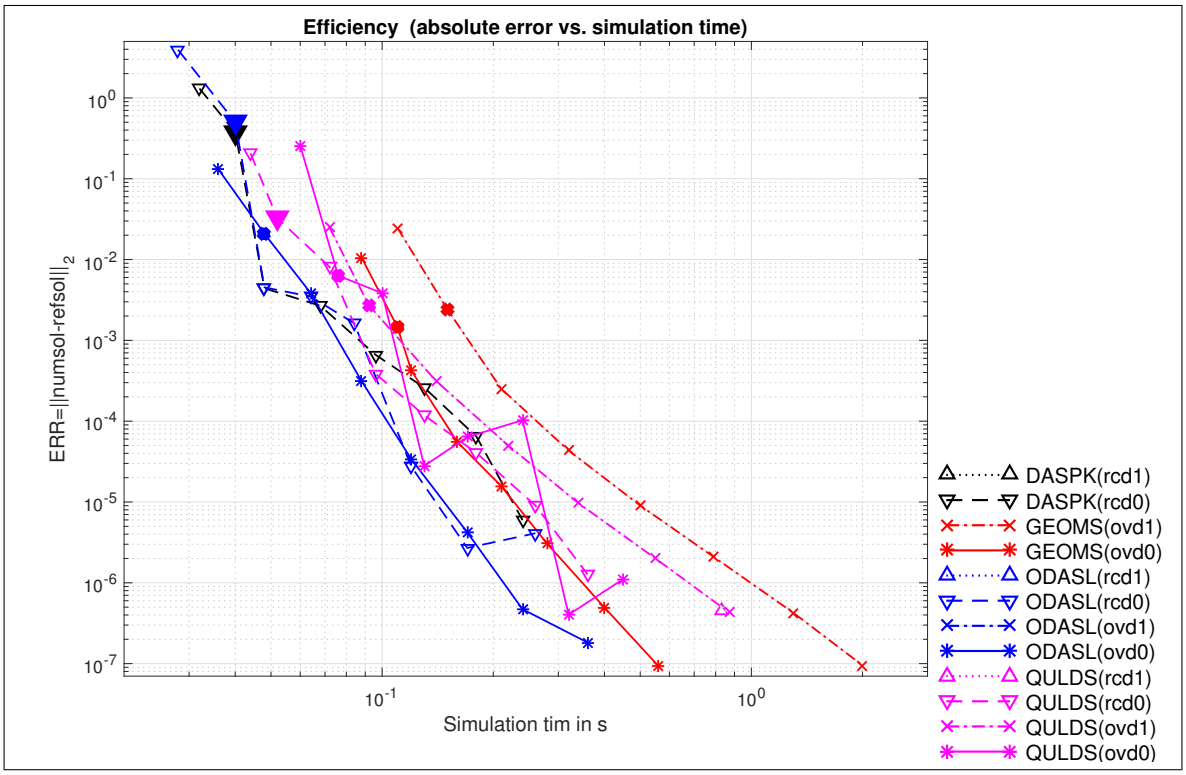

Figure 8: Scenario 01: Efficiency

2.2.2 Scenario 02

This Scenario 02 is almost the same as Scenario 01 except the length l_1 is increased to 2.99m such that both arms have almost the same length. Note that in case of same arm lengths the slider crank passes a singular position if both arms are in vertical position. In this case there exists a bifurcation since the both arms can either rotate together around the suspension and the mass remains in the origin or the mass moves horizontally such the both arms straddle.

m_1	$= 1$ kg	l_1	$= 2.99$ m	$\mathfrak{g}$	$= 9.81$ m/s^2
m_2	$= 1.8$ kg	l_1	$= 3$ m		

Table 7: Scenario 01: Parameters

We have the equations of motion given in (1), the parameters as depicted in Table 7, and the initial values (11) fit also in this scenario.

Reference Solution As in the previous scenario 01 this problem is not analytically solvable. Therefore, we use the numerical solution obtained with `QUALIDAES` for the overdetermined c-level 0 formulation (ovd0) with a prescribed tolerance `ATOL`=`RTOL`=10^{-11} as reference solution for comparisons of the obtained precision.

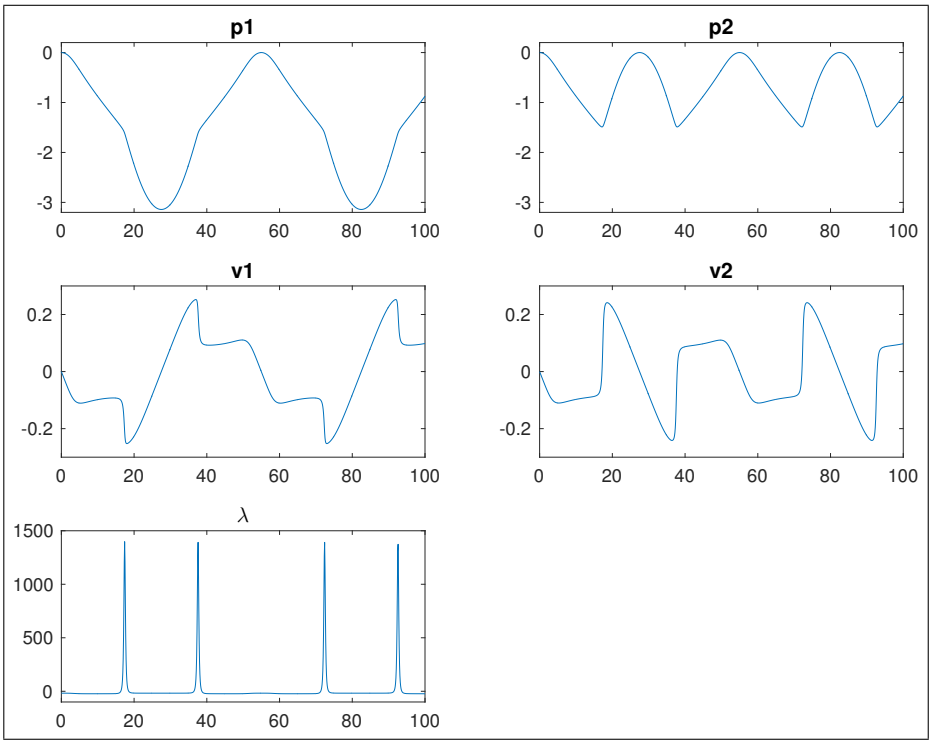

Figure 9: Scenario 02: Analytical solution

In Figure 9 the reference solution is illustrated, while in Figure 10 the reference solution for the first 20s is illustrated. Furthermore, in Table 8 the values of the reference solution at the final time $t_f = 100$s are listed.

$x(t_f) =$	-0.8741612302108804D+00	$y(t_f) =$	-0.8701860569010188D+00
$v(t_f) =$	0.9836442284414978D-01	$w(t_f) =$	0.9757365803459964D-01
$\lambda(t_f) =$	-0.2310397315625302D+02		

Table 8: Scenario 02: Reference solution at the final time point $t_f = 100$s.

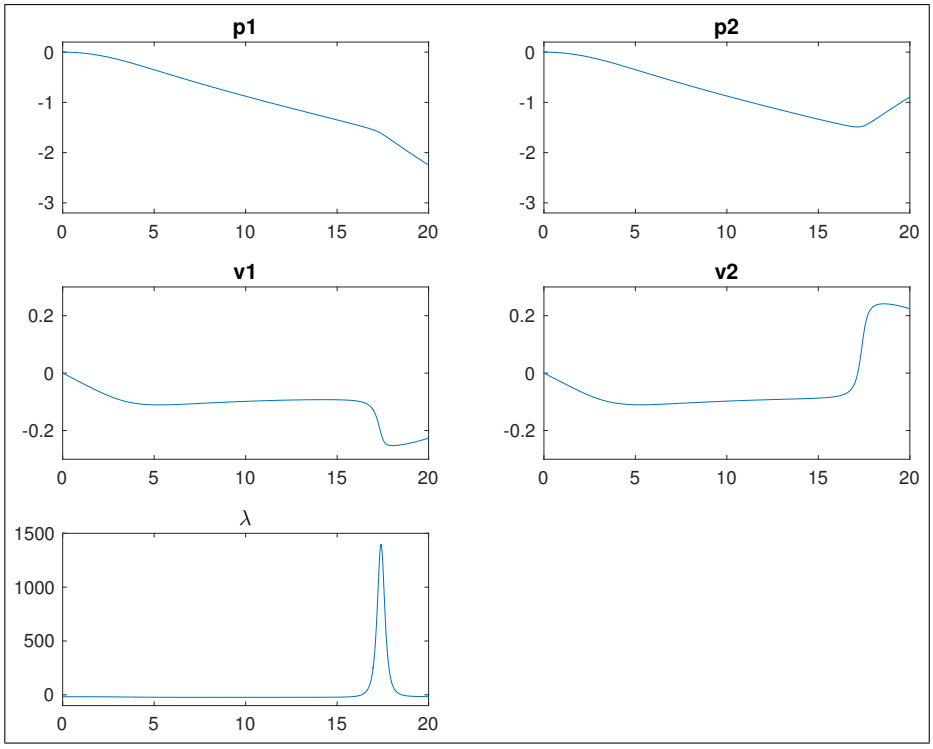

Figure 10: Scenario 02: Reference solution for the first 20s only, i.e., $\mathbb{I} = [0\text{s}, 20\text{s}]$

Numerical Solution For the numerical computations the tolerances RTOL=ATOL=10^{-i}, $i = 5, ..., 10$ are prescribed uniformly for all components of the state variables. Selected driver subroutines for the used solver-formulation combinations are available on the webpage `http://www3.math.tu-berlin.de/multiphysics/Examples/M002_SliderCrank/`. The used solver-formulation combinations and an overview of the success is illustrated in Table 9. Here it can be seen that the numerical integration using the the d-index 2 formulation (rcd1) was only successful for some prescribed tolerances with QUALIDAES. Furthermore, the numerical integration using the the overdetermined c-level 1 formulation (ovd1) was only successful for some prescribed tolerances with GEOMS and QUALIDAES. The difficulty in the numerical integration of (rcd1) and (ovd1) is due to the existence of hidden constraints. Note that GEOMS internally uses a scaling of the unknown variables due to the special structure of the equations of motion for multibody systems. Furthermore, GEOMS is not applicable to the d-index 2 or d-index 1 formulations since GEOMS requires the multibody structure in the model equations. All numerical integrations based on the d-index 1 formulation (rcd0) were successful independent of the used numerical method.

	rcd1	rcd0	ovd1	ovd0
DASPK	o[1]	X	-[4]	-[4]
GEOMS	-[5]	-[5]	x	X
ODASSL	o[1]	X	o[1]	X
QUALIDAES	x	X	x	X

'X' successful for every prescribed tolerance
'x' successful for some/few prescribed tolerances
'o' not successful for every prescribed tolerance
'-' formulation does not satisfy the structural requirements of the solver

[1] not suitable for DAEs consisting hidden constraints (c-level>0)
[2] not suitable for DAEs consisting hidden constraints of higher level than 1 (c-level>1)
[4] not suitable for overdetermined DAEs
[5] GEOMS is only suited for MBS structure including at least hidden constraints on velocity level

Table 9: Scenario 02: Used solver-formulation combinations and an overview of the success

In Figure 11 we have illustrated the solution of the numerical integration for the whole time domain $\mathbb{I}$ by use of the solver-formulation combinations with a prescribed tolerance RTOL=ATOL=10^{-6}. In Figure 12 these solution of the numerical integration are illustrated for the time domain $[0\text{s}, 20\text{s}]$. Furthermore, in Figure 13 the obtained error of these numerical solutions is illustrated in logarithmic style. The largest

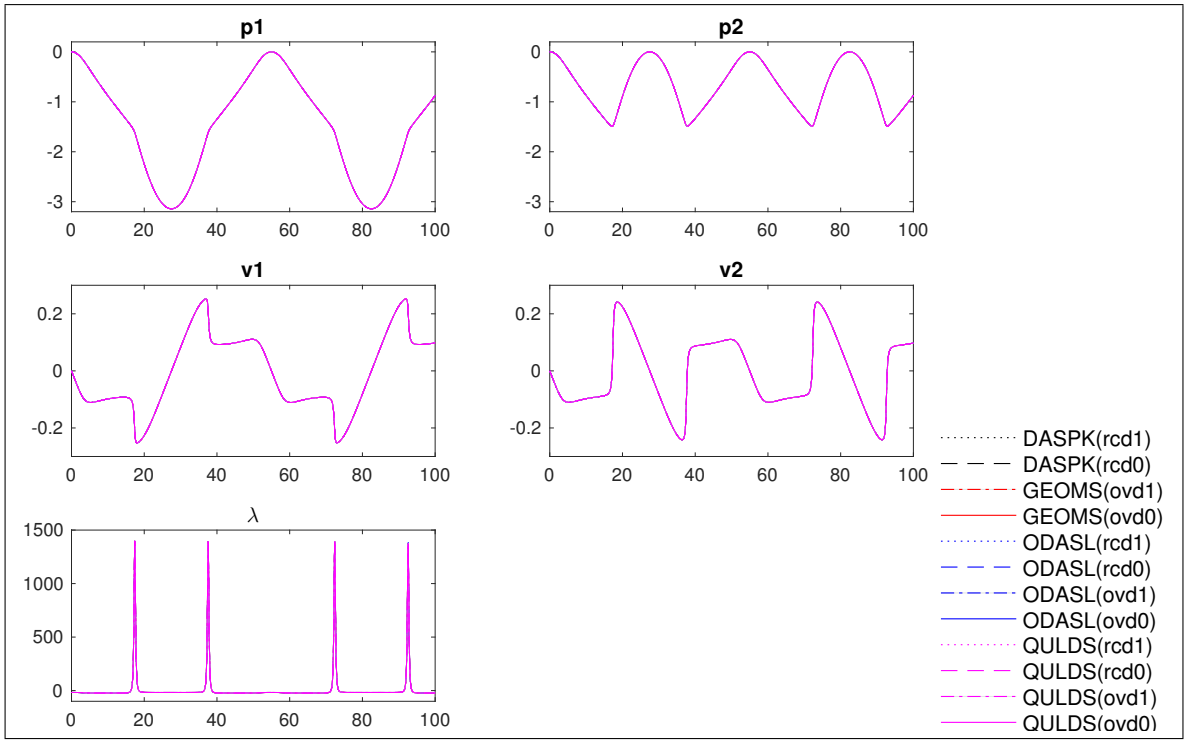

Figure 11: Scenario 02: Numerical solutions for a prescribed tolerance of RTOL=ATOL=10^{-6}

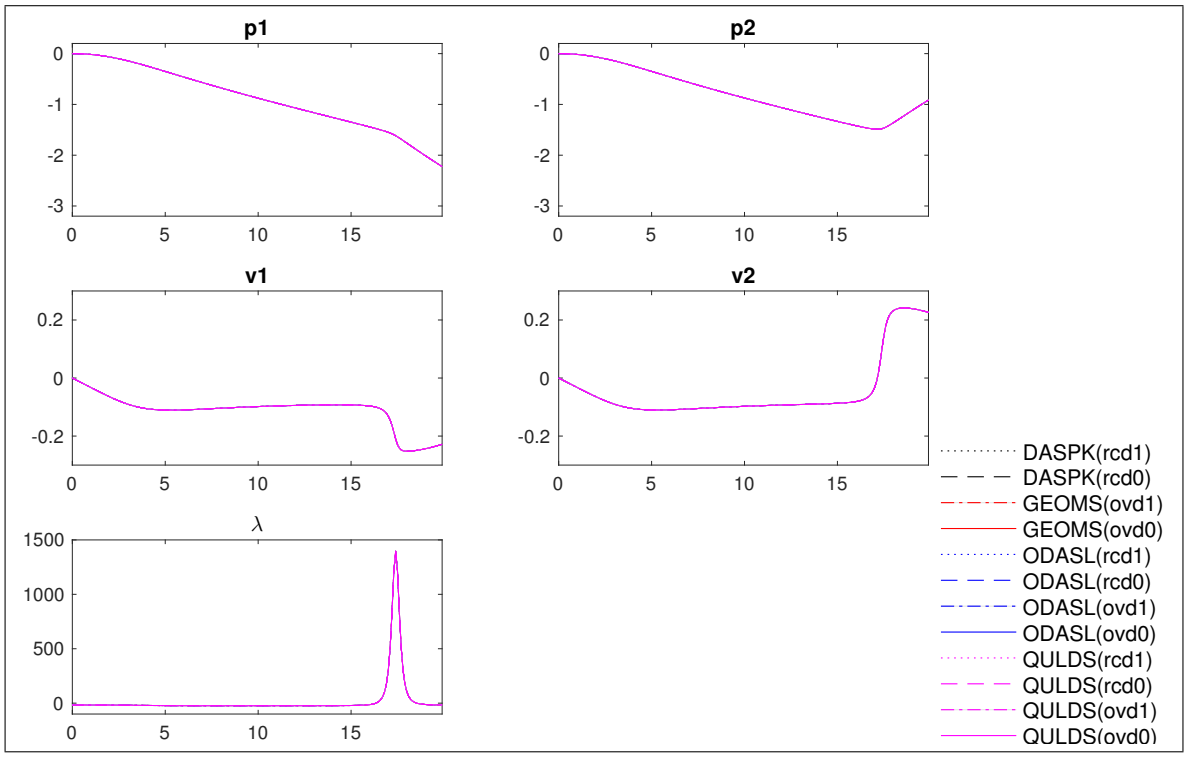

Figure 12: Scenario 02: Numerical solutions (zoom) for a prescribed tolerance of RTOL=ATOL=10^{-6}

deviation show the solutions DASPK(rcd0) and ODASSL(rcd0) which mainly comes from the drift due to the missing constraints (1c) and (6a) in the d-index 1 formulation (rcd0) (8) which leads up to quadratic drift from the constraints of position level (1c) and linear drift from the constraints of velocity level (6a), as illustrated in Figure 14. The best accuracy for the prescribed tolerance RTOL=ATOL=10^{-6} is obtained by the usage of the solvers QUALIDAES(rcd1) and QUALIDAES(ovd1).

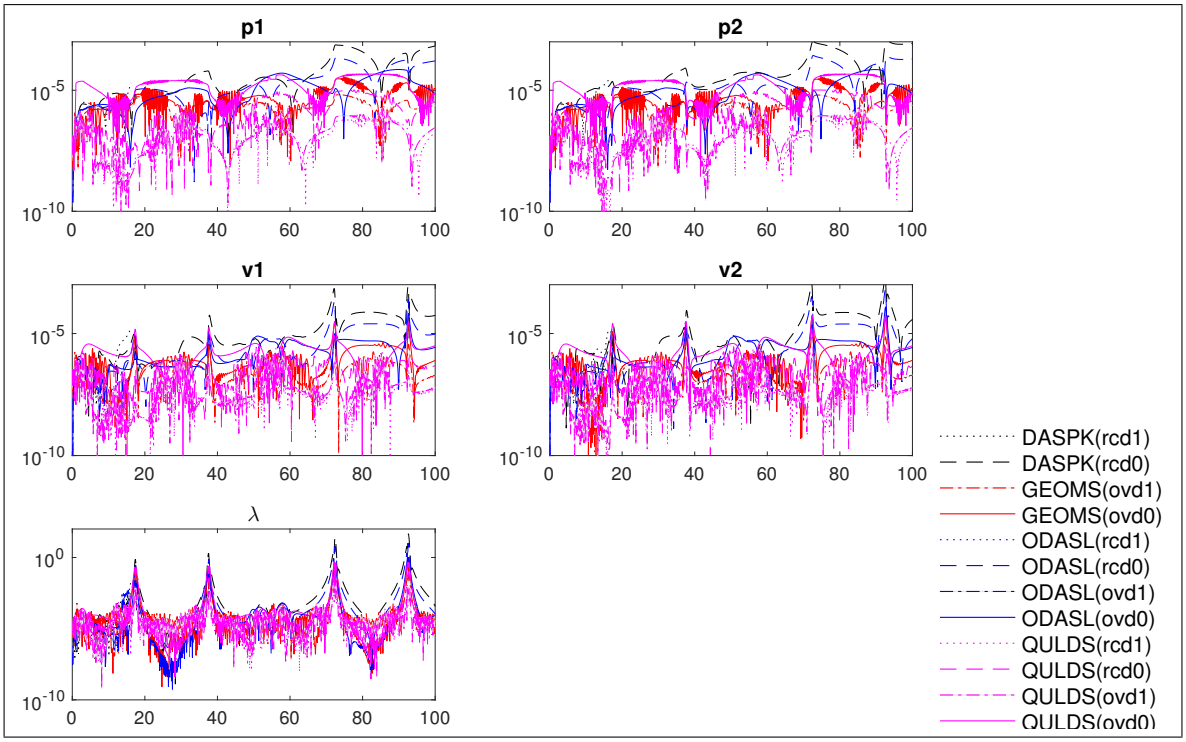

Figure 13: Scenario 02: Numerical error for a prescribed tolerance of RTOL=ATOL=10^{-6}

In Figure 14 we have illustrated the absolute residuals of the constraints, including the hidden constraints, as well as the energy conserving constraint for the numerical results. The numerical solutions show the behavior depending on the used formulations as expected in the regulatrizations, see Section 2.1.4. So the constraint on position level (1c) is mainly violated with a large deviation from DASPK(rcd0), ODASSL(rcd0), and QUALIDAES(rcd0). Furthermore, the numerical results DASPK(rcd0) and ODASSL(rcd0) show large deviation in the beginning of the time integration until the abort of the numerical integration. This deviation is caused by the (expected) drift off effect and the higher index of the used formulation (rcd1). The other violation of the constraints of position level for the other solver-formulation combinations fits into the prescribed tolerance of 10^{-6}. In particular note that also QUALIDAES(rcd1) yields precise results which would not be excepted.
The constraints on velocity level are significantly violated for DASPK(rcd0) and ODASSL(rcd0). The other violations of the constraints of position level for the other solver-formulation combinations fits into the prescribed tolerance of 10^{-6}.
The energy conservation is obtained very good for the numerical results obtained with QUALIDAES(rcd1) and for the solver-formulation combination QUALIDAES(ovd1) followed by GEOMS(ovd1). The numerical results DASPK(rcd0), ODASSL(ovd0) and QUALIDAES(ovd0) conserve the energy not very precise.
Details in the efficiency for all computations with at least one successful run are listed in Table 10 and illustrated in Figure 15 for a selection of the numerical results. For this scenario the numerical solutions from ODASSL with the overdetermined c-level 0 formulation (ovd0) (10) offer the best efficiency. is very efficient, slightly behind followed by QUALIDAES(rcd1), QUALIDAES(ovd1), QUALIDAES(rcd0), DASPK(rcd0), and GEOMS(ovd1). The increased time consume of QUALIDAES(ovd0) and GEOMS(ovd0) is due to the increased size of the overdetermined c-level 0 formulation and the application of a Runge-Kutta method. Nevertheless, GEOMS and QUALIDAES are the only solver which are able to integrate a formulation (here (ovd1) and (rcd1)) still containing hidden constraints. The most precise results are obtained by ODASSL(ovd0), GEOMS(ovd0), and ODASSL(ovd0). For quantitative details in the efficiency, see Table 10.

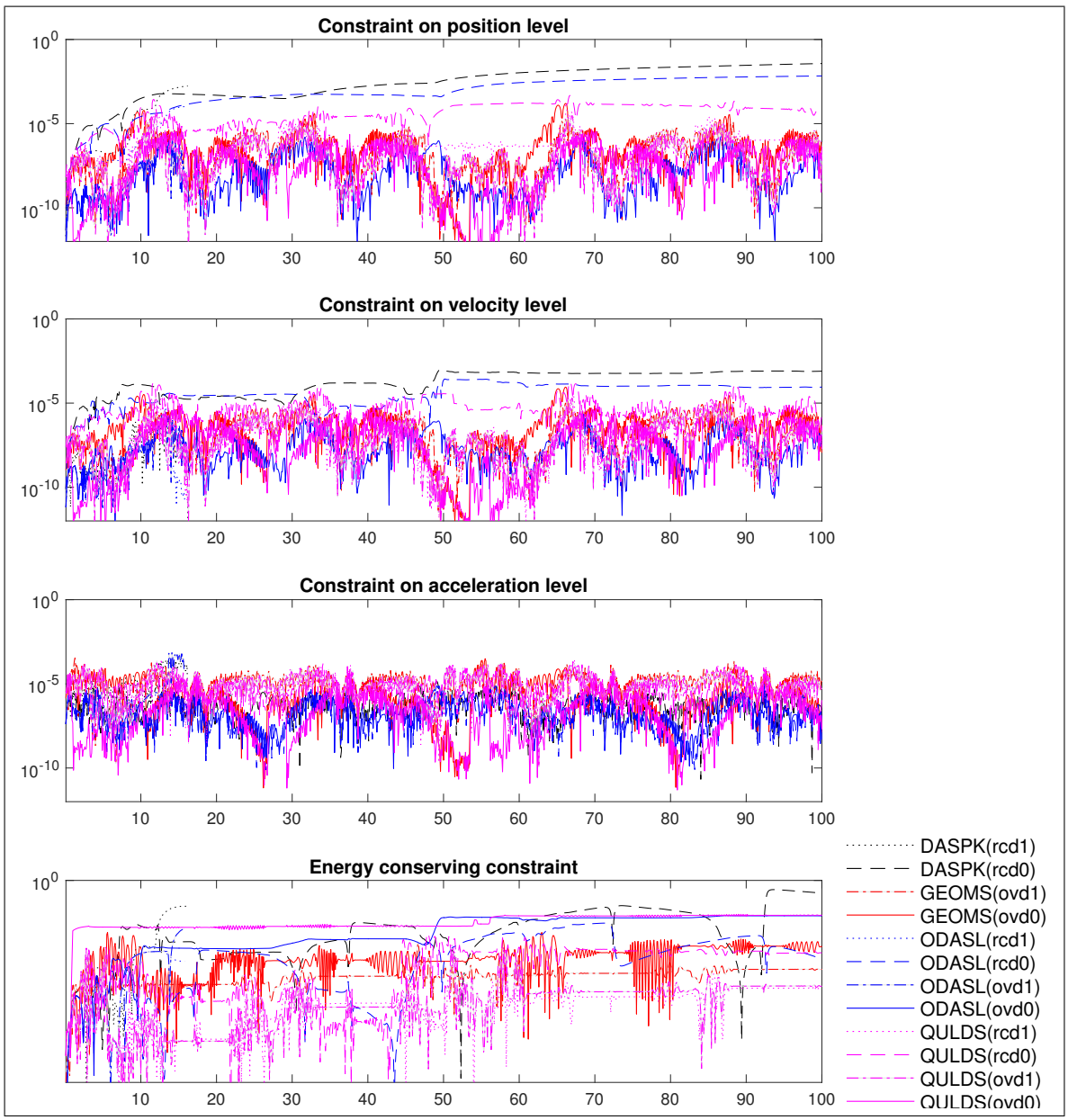

Figure 14: Scenario 02: Residuum of the constraints for a prescribed tolerance of RTOL=ATOL=10^{-6}

	Tol	10^{-5}	10^{-6}	10^{-7}	10^{-8}	10^{-9}	10^{-10}
DASPK(rcd0)	Tsim	8.0e-03	2.0e-02	2.0e-02	3.2e-02	3.2e-02	4.0e-02
	ERR	1.3e+02	2.6e+01	1.7e+00	5.9e-01	8.8e-03	4.8e-03
GEOMS(ovd1)	Tsim	2.8e-02	3.6e-02	4.8e-02	8.0e-02	1.2e-01	-
	ERR	1.4e+00	1.1e-01	3.0e-03	4.8e-04	8.6e-05	-
GEOMS(ovd0)	Tsim	4.8e-02	5.6e-02	6.4e-02	8.0e-02	9.2e-02	9.6e-02
	ERR	4.1e+00	3.9e-01	3.5e-02	3.2e-03	4.7e-04	6.6e-05
ODASSL(rcd0)	Tsim	1.2e-02	1.6e-02	1.6e-02	2.0e-02	2.4e-02	3.6e-02
	ERR	3.6e+01	6.2e+00	5.5e-01	8.5e-02	8.7e-03	4.1e-03
ODASSL(ovd0)	Tsim	1.6e-02	1.6e-02	2.0e-02	2.0e-02	3.2e-02	4.0e-02
	ERR	1.9e+00	7.1e-01	5.2e-02	1.1e-02	8.3e-04	4.4e-05
QUALIDAES(rcd1)	Tsim	1.6e-02	2.4e-02	3.2e-02	4.8e-02	6.8e-02	-
	ERR	1.1e-01	1.2e-02	2.3e-03	5.7e-04	3.2e-04	-
QUALIDAES(rcd0)	Tsim	1.6e-02	1.6e-02	2.0e-02	2.4e-02	2.8e-02	4.0e-02
	ERR	6.2e+01	1.2e-01	1.2e+00	1.3e-01	8.4e-03	1.2e-03
QUALIDAES(ovd1)	Tsim	1.6e-02	2.4e-02	3.6e-02	4.8e-02	7.2e-02	-
	ERR	1.8e-01	9.4e-03	3.9e-03	5.2e-04	1.3e-04	-
QUALIDAES(ovd0)	Tsim	4.0e-02	4.4e-02	5.2e-02	6.4e-02	7.6e-02	1.0e-01
	ERR	6.2e+01	4.8e-01	4.3e-02	1.3e-02	1.4e-03	8.9e-05

Tsim - Simulation time in seconds, ERR - error w.r.t. reference solution, '-' numerical integration was not successful

Table 10: Scenario 02: Efficiency

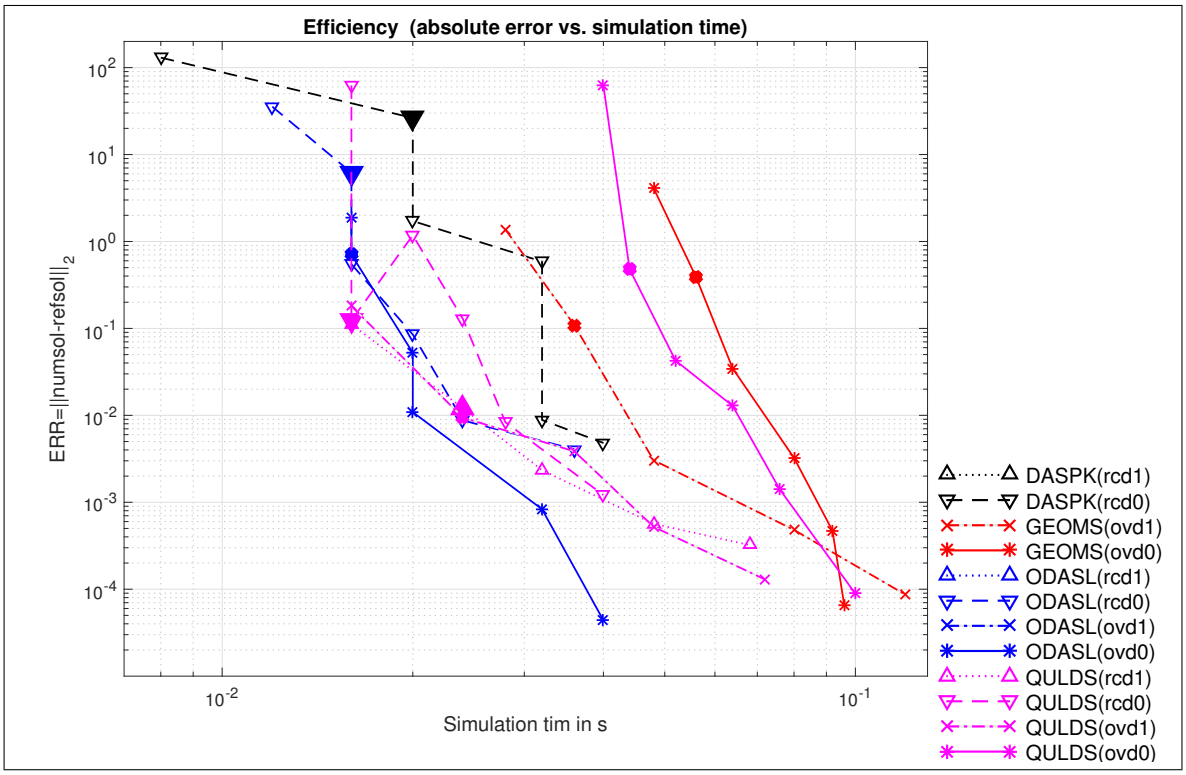

Figure 15: Scenario 02: Efficiency

2.2.3 Scenario 03

This Scenario 03 is almost similar to the previous scenarios except that
· the time domain is extended to $\mathbb{I} = [0\text{s}, 1000\text{s}]$
· the mass m_1 is decreased to 10^{-4}kg (almost zero), and
· the length l_2 is increased to 300m.

m_1	$= 10^{-4}$ kg	l_1	$= 1$ m	$\mathfrak{g}$	$= 9.81$ m/s^2
m_2	$= 1.8$ kg	l_1	$= 300$ m		

Table 11: Scenario 03: Parameters

We have the equations of motion given in (1), the parameters as depicted in Table 11, and the initial values (11) fit also in this scenario.

Reference Solution As in the previous scenarios this problem is not analytically solvable. Therefore, we use the numerical solution obtained with `GEOMS` for the overdetermined c-level 0 formulation (ovd0) with a prescribed tolerance `ATOL`=`RTOL`=10^{-14} as reference solution for comparisons of the obtained precision.

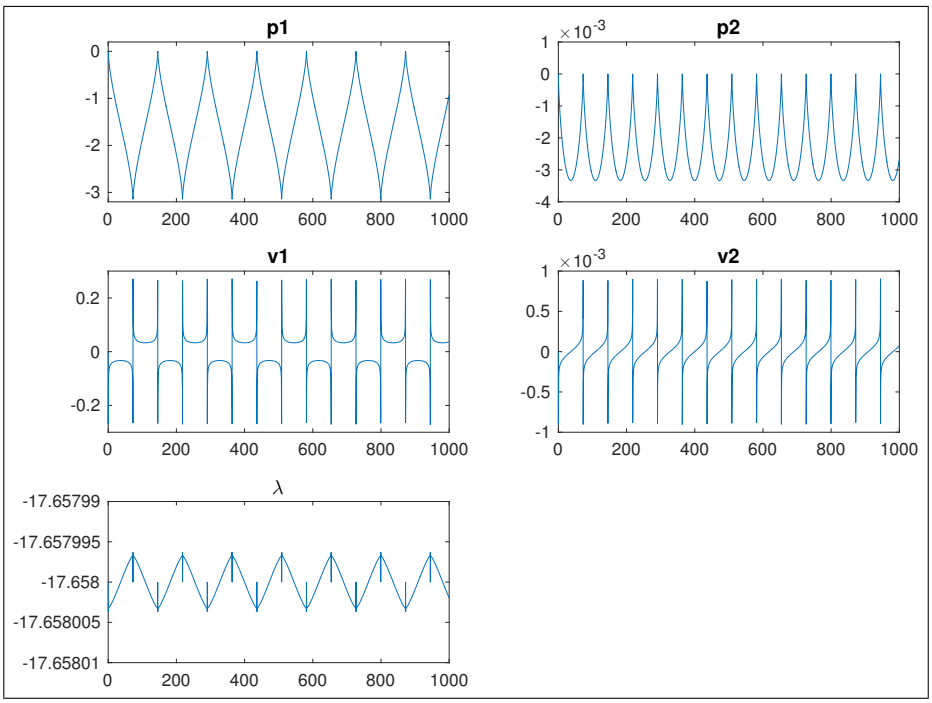

Figure 16: Scenario 03: Reference solution

In Figure 16 the reference solution is illustrated, while in Figure 17 the reference solution for the first second and in Figure 18 the reference solution for the 73rd second is illustrated. Furthermore, in Table 12 the values of the reference solution at the final time $t_f = 1000$s are listed.

$x(t_f) =$	-0.9230130214808158D+00	$y(t_f) =$	-0.2658080980291223D-02
$v(t_f) =$	0.3689582388107326D-01	$w(t_f) =$	0.7421255253566746D-04
$\lambda(t_f) =$	-0.1765800196940036D+02		

Table 12: Scenario 03: Reference solution at the final time point $t_f = 1000$s.

Numerical Solution For the numerical computations the tolerances `RTOL`=`ATOL`=10^{-i}, $i = 5, ..., 12$ are prescribed uniformly for all components of the state variables. Selected driver subroutines for the

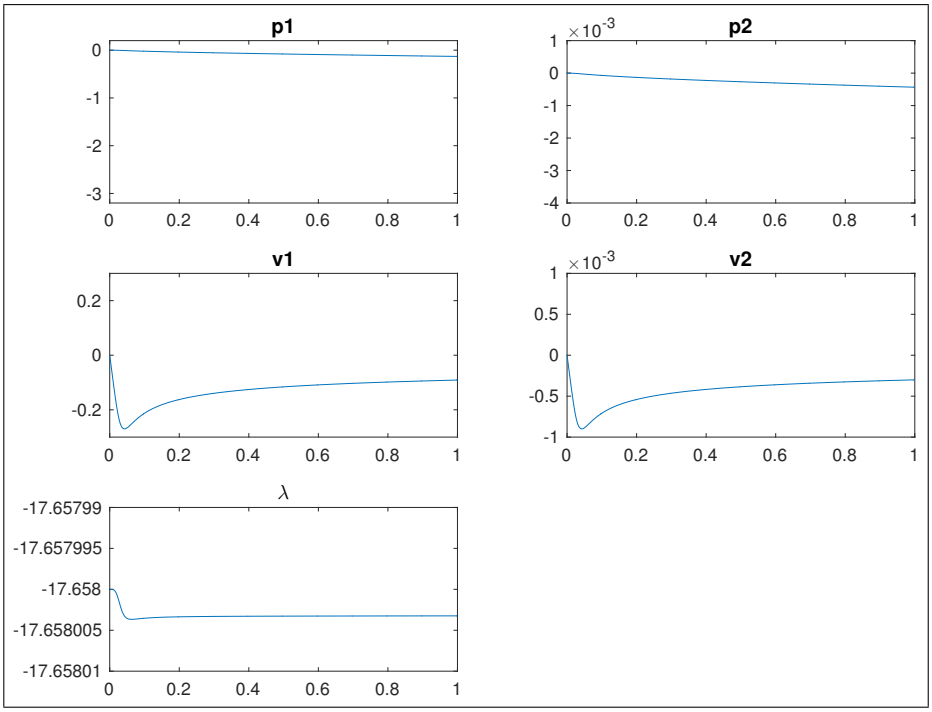

Figure 17: Scenario 03: Reference solution for the first second only, i.e., $\mathbb{I} = [0\text{s}, 1\text{s}]$

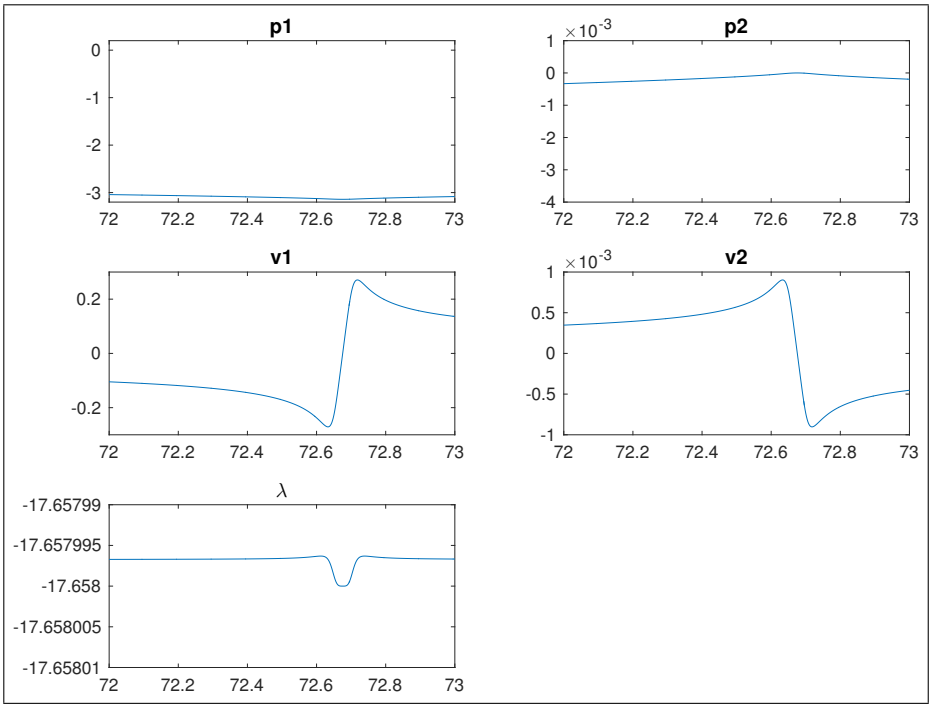

Figure 18: Scenario 03: Reference solution for the 73rd second only, i.e., $\mathbb{I} = [72\text{s}, 73\text{s}]$

used solver-formulation combinations are available on the webpage
`http://www3.math.tu-berlin.de/multiphysics/Examples/M002_SliderCrank/`. The used solver-formulation combinations and an overview of the success is illustrated in Table 13. Here it can be seen that computations for some prescribed tolerances only for the d-index 2 formulation (rcd1) and the overdetermined c-level 1 formulation (ovd1) which still contain hidden constraints were not successful with `DASPK` and `ODASSL`. Furthermore, the numerical integration performed by `GEOMS` and `QUALIDAES` were successful for every prescribed tolerance and every provided formulation of the model equations.

	rcd1	rcd0	ovd1	ovd0
DASPK	x[1]	X	-[4]	-[4]
GEOMS	-[5]	-[5]	X	X
ODASSL	x[1]	X	x[1]	X
QUALIDAES	X	X	X	X

'X' successful for every prescribed tolerance
'x' successful for some/few prescribed tolerances
'o' not successful for every prescribed tolerance
'-' formulation does not satisfy the structural requirements of the solver

[1] not suitable for DAEs consisting hidden constraints (c-level>0)
[2] not suitable for DAEs consisting hidden constraints of higher level than 1 (c-level>1)
[4] not suitable for overdetermined DAEs
[5] GEOMS is only suited for MBS structure including at least hidden constraints on velocity level
[6] the leading matrix of a quasi-linear DAE is required to be constant

Table 13: Scenario 03: Used solver-formulation combinations and an overview of the success

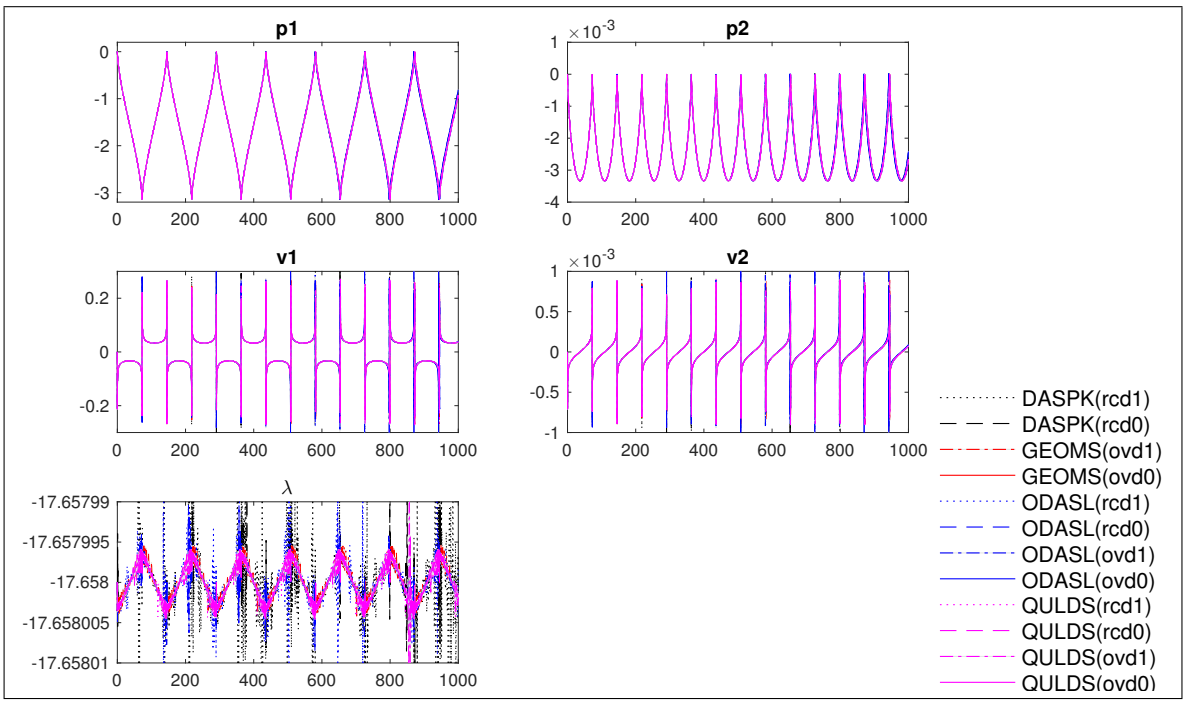

Figure 19: Scenario 03: Numerical solutions for a prescribed tolerance of RTOL=ATOL=10^{-6}

In Figure 19 we have illustrated the solution of the numerical integration for the whole time domain $\mathbb{I}$ by use of the solver-formulation combinations with a prescribed tolerance RTOL=ATOL=10^{-6}. In Figure 20 these solution of the numerical integration are illustrated for the time domain $[0\text{s}, 100\text{s}]$. Furthermore, in Figure 21 the obtained error of these numerical solutions is illustrated in logarithmic style. The largest deviation is shown from the solutions ODASSL(ovd0) and ODASSL(ovd1) slightly followed by DASPK(rcd0) and DASPK(rcd1). The best accuracy for the prescribed tolerance is obtained by the usage of the solvers QUALIDAES(ovd1) and QUALIDAES(ovd0). and also slightly reduced for QUALIDAES(rcd1) and GEOMS(ovd1).

In Figure 22 we have illustrated the absolute residuals of the constraints, including the hidden constraints, as well as the energy conserving constraint for the numerical results. The numerical solutions show the behavior depending on the used formulations as expected in the regulatrizations, see Section 2.1.4. So the constraint on position level (1c) is mainly violated with a large deviation for DASPK(rcd0), ODASSL(rcd0), and QUALIDAES(rcd0). A significant deviation is obtained for DASPK(rcd1), ODASSL(rcd1), and QUALIDAES(rcd1). These deviations are caused by the (expected) drift off effect in quadratic manner for (rcd0) and linear manner for (rcd1). The violation of the constraints of position level for the other solver-formulation combinations fits into the prescribed tolerance of 10^{-6}.
The constraints on velocity level are significantly violated for DASPK(rcd0) and ODASSL(rcd0). The other violation of the constraints of position level for the other solver-formulation combinations fits into the prescribed tolerance of 10^{-6}.
The constraint on acceleration level is preserved for all numerical integrations within the prescribed tol-

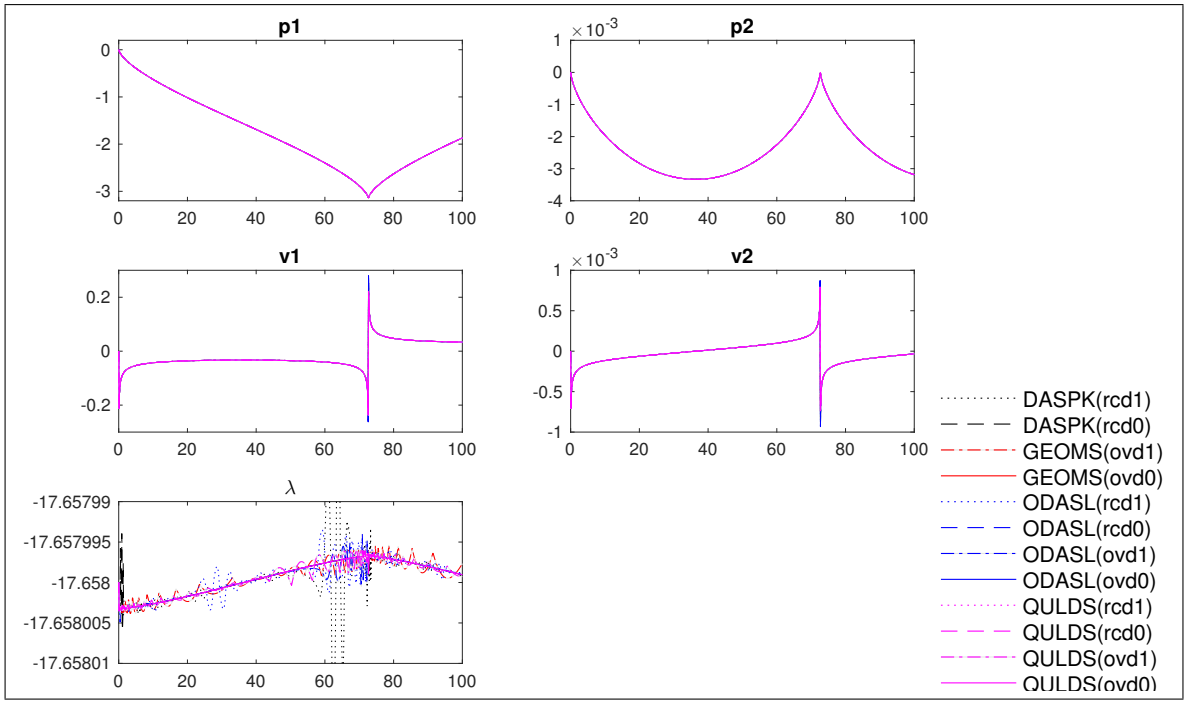

Figure 20: Scenario 03: Numerical solutions (zoom) for a prescribed tolerance of RTOL=ATOL=10^{-6}

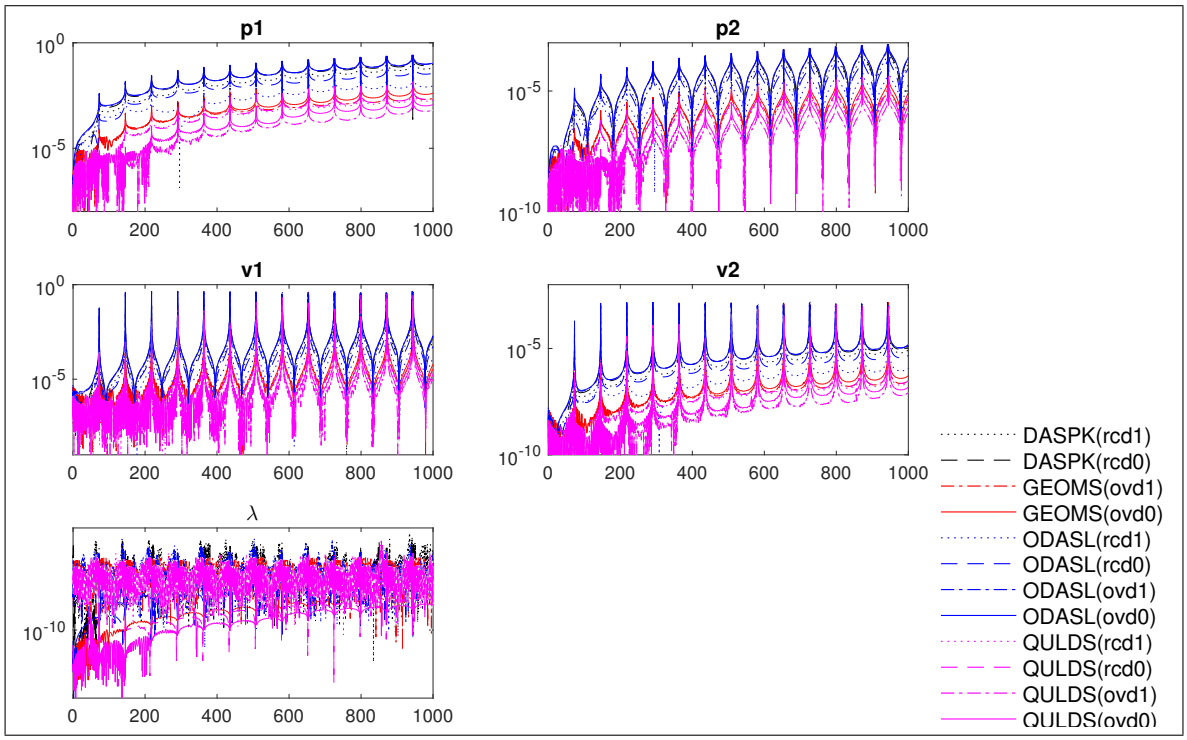

Figure 21: Scenario 03: Numerical error for a prescribed tolerance of RTOL=ATOL=10^{-6}

erance.

The energy conservation is obtained very good for the numerical results obtained with GEOMS(ovd0), ODASSL(ovd0), and QUALIDAES(ovd0) as well as GEOMS(ovd1), ODASSL(ovd1), and QUALIDAES(ovd1). Furthermore, the energy conservation is obtained acceptable for the numerical results obtained with DASPK(rcd1), ODASSL(rcd1), and QUALIDAES(rcd1) as well as for QUALIDAES(rcd0). The numerical results DASPK(rcd0) and ODASSL(ovd0) conserve the energy not very precise.

Details in the efficiency for all computations with at least one successful run are listed in Table 14

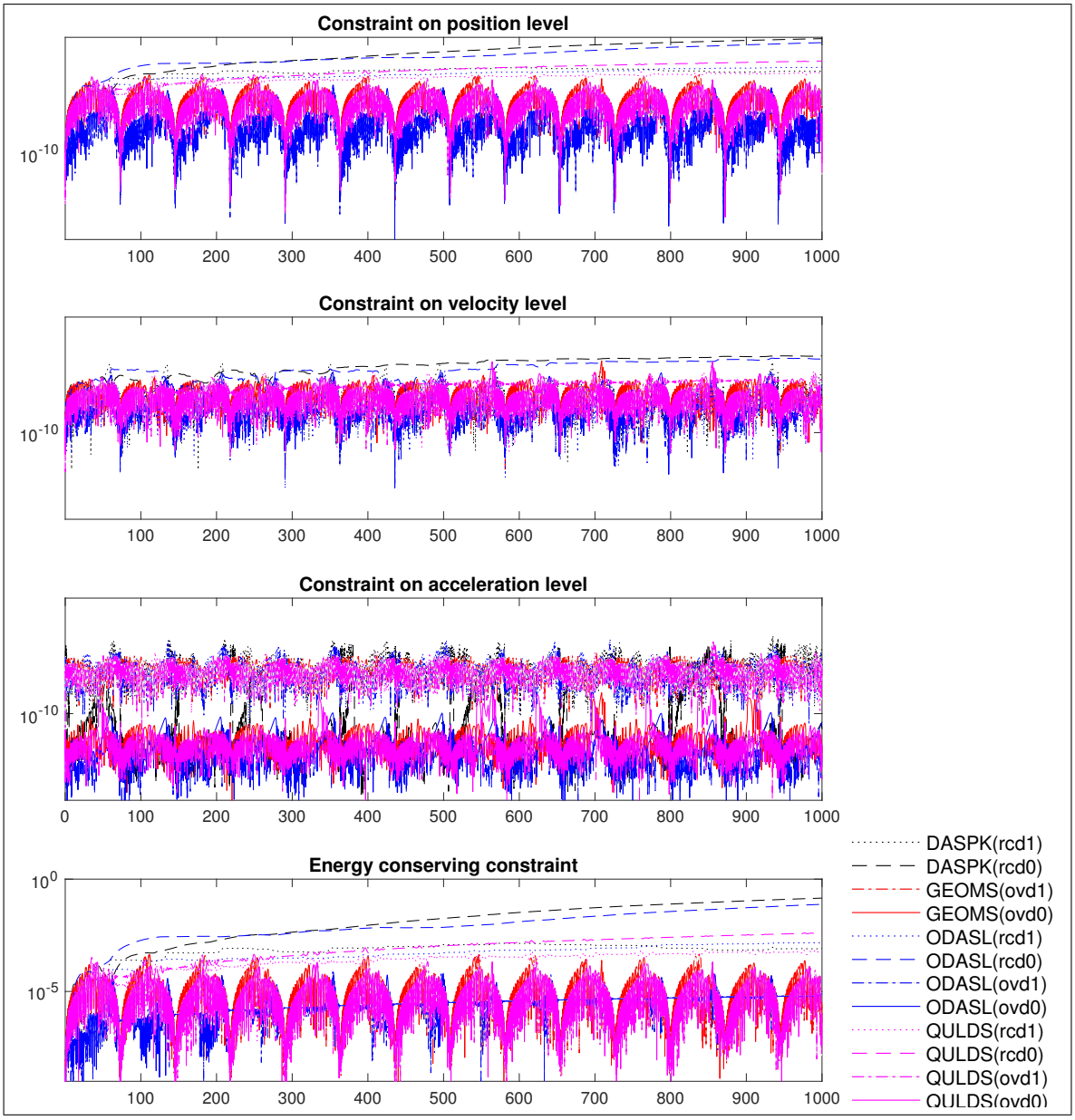

Figure 22: Scenario 03: Residuum of the constraints for a prescribed tolerance of RTOL=ATOL=10^{-6}

and illustrated in Figure 23 for the numerical results. For this scenario the numerical solutions from QUALIDAES with all used formulations offers the best efficiency. The efficiency of ODASSL(rcd1) is also very good, followed by GEOMS(ovd1), ODASSL(rcd0), DASPK(rcd0), and GEOMS(ovd0). The most precise results are obtained by QUALIDAES(ovd1) and GEOMS(ovd1). For quantitative details in the efficiency, see Table 14.

	Tol	10^{-5}	10^{-6}	10^{-7}	10^{-8}	10^{-9}	10^{-10}	10^{-11}	10^{-12}
DASPK(rcd1)	Tsim	1.0e-01	1.0e-01	1.0e-01	1.2e-01	1.4e-01	-	-	-
	ERR	5.3e+00	1.4e+00	4.8e-01	1.4e-01	2.2e-02	-	-	-
DASPK(rcd0)	Tsim	9.6e-02	9.6e-02	1.0e-01	1.1e-01	1.2e-01	1.3e-01	1.6e-01	2.0e-01
	ERR	5.0e+00	1.9e+00	6.3e-01	2.4e-01	4.1e-02	6.7e-03	9.1e-04	1.3e-04
GEOMS(ovd1)	Tsim	1.0e-01	1.0e-01	1.1e-01	1.3e-01	1.4e-01	1.7e-01	2.1e-01	2.8e-01
	ERR	6.0e-01	2.1e-01	4.3e-02	6.2e-03	9.7e-04	1.3e-04	2.0e-05	2.4e-06
GEOMS(ovd0)	Tsim	1.0e-01	1.0e-01	1.2e-01	1.3e-01	1.5e-01	1.7e-01	2.1e-01	2.7e-01
	ERR	7.6e-01	2.5e-01	4.7e-02	6.2e-03	4.5e-03	9.1e-04	1.7e-04	2.3e-05
ODASSL(rcd1)	Tsim	9.2e-02	9.6e-02	1.0e-01	1.1e-01	1.2e-01	1.5e-01	-	-
	ERR	2.5e+00	4.8e-01	8.3e-02	3.4e-02	1.6e-03	8.3e-05	-	-
ODASSL(rcd0)	Tsim	8.8e-02	9.6e-02	1.0e-01	1.1e-01	1.2e-01	1.4e-01	1.7e-01	2.1e-01
	ERR	1.0e+01	9.3e-01	3.1e-01	6.0e-02	2.1e-02	1.5e-03	1.5e-04	1.7e-05
ODASSL(ovd1)	Tsim	1.0e-01	1.0e-01	1.0e-01	1.2e-01	1.3e-01	1.5e-01	1.9e-01	-
	ERR	6.9e+00	2.1e+00	6.7e-01	2.2e-01	3.7e-02	5.8e-03	7.3e-04	-
ODASSL(ovd0)	Tsim	1.0e-01	1.0e-01	1.0e-01	1.2e-01	1.4e-01	1.6e-01	1.9e-01	2.4e-01
	ERR	6.3e+00	2.0e+00	6.9e-01	2.2e-01	3.4e-02	5.5e-03	8.2e-04	1.2e-04
QUALIDAES(rcd1)	Tsim	8.4e-02	9.2e-02	9.2e-02	1.0e-01	1.1e-01	1.2e-01	1.4e-01	1.8e-01
	ERR	7.3e-01	1.7e-01	3.6e-02	2.4e-03	5.4e-04	1.1e-04	1.5e-05	1.1e-06
QUALIDAES(rcd0)	Tsim	8.8e-02	8.8e-02	9.2e-02	1.0e-01	1.1e-01	1.2e-01	1.4e-01	1.7e-01
	ERR	7.4e-01	1.8e-01	7.1e-02	1.3e-02	1.1e-02	2.0e-03	7.8e-05	2.1e-05
QUALIDAES(ovd1)	Tsim	8.4e-02	8.8e-02	9.2e-02	1.0e-01	1.1e-01	1.2e-01	1.4e-01	1.8e-01
	ERR	7.3e-01	5.8e-02	2.6e-02	4.4e-03	7.1e-04	1.1e-04	1.5e-05	1.1e-06
QUALIDAES(ovd0)	Tsim	8.8e-02	9.2e-02	9.6e-02	1.0e-01	1.1e-01	1.3e-01	1.5e-01	1.8e-01
	ERR	7.0e-01	1.1e-01	2.3e-02	4.8e-03	2.1e-03	3.5e-04	8.4e-05	1.4e-05

Tsim - Simulation time in seconds, ERR - error w.r.t. reference solution, '-' numerical integration was not successful

Table 14: Scenario 03: Efficiency

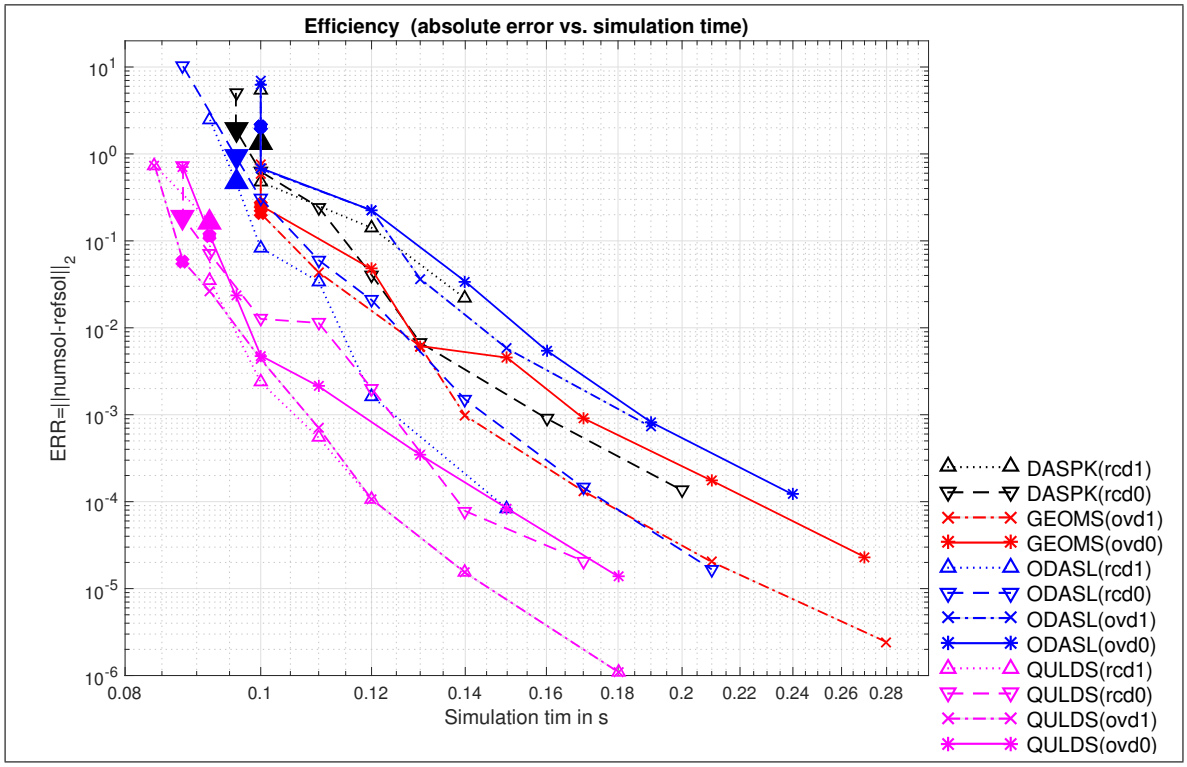

Figure 23: Scenario 03: Efficiency

2.2.4 Scenario 04

In this scenario, let us consider the case that both arms of the slider crank have the same length, say $l_1 = l_2 = 1$, see Table 15. In particular, we will simulate the motion of the slider crank on $\mathbb{I} = [0\text{s}, 2\text{s}]$ with the parameters as depicted in Table 15 and the initial values (11) which fit also in this scenario. The equations of motion are given in (1).

m_1	$= 1$ kg	l_1	$= 1$ m	$\mathfrak{g}$	$= 9.81$ m/s^2
m_2	$= 1.8$ kg	l_2	$= 1$ m		

Table 15: Scenario 04: Parameters

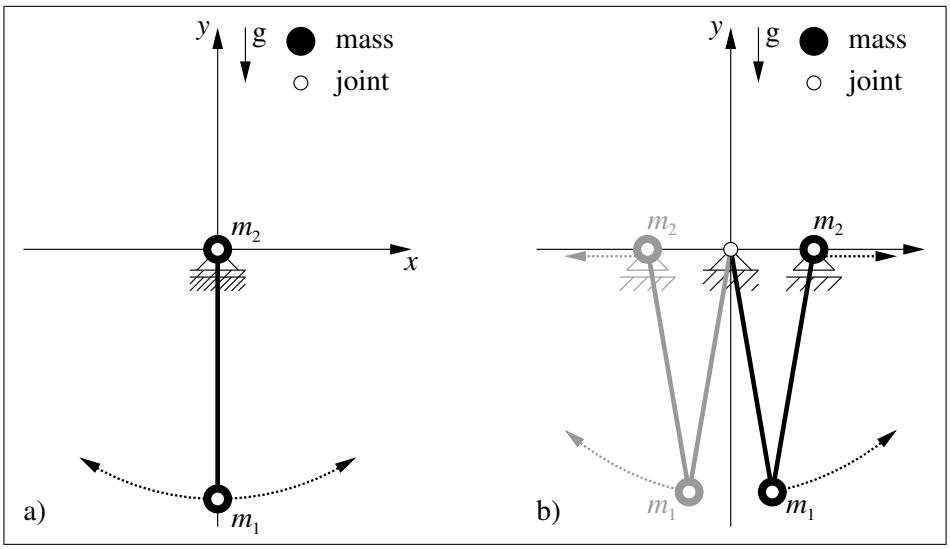

Figure 24: Scenario 04: Singular position and possible motion after the bifurcation.

In this case of $l_1 = l_2 = 1$ the motion of the slider crank passes the state $p_1 = p_2 = -\pi/2$, where both arms of the slider crank are hanging down over each other (see a) in Figure 24) and the end of the second rod is placed in the origin. In this scenario, this state is reached at (approximately) $t = 1.012s$. In this situation the rank of the constraint matrix G jumps from 1 to 0 such that we have reached a singularity. Then the constraints are redundant and there is a singular point in the solution path such that the further solution is not uniquely determined. Two motions are possible. First, the end of the slider crank remains in the point of origin and both rods are rotating around it (see a) in Figure 24), or secondly, the end of the slider crank moves to the left or to the right and the angle between the arms increases (see b) in Figure 24).
The obtained numerical solutions for the position p_1 and for the velocity v_1 for a prescribed tolerance `RTOL`=`ATOL`=10^{-6} over the time domain $\mathbb{I} = [0\text{s}, 2\text{s}]$ with the solver-formulation combinations are presented in Figures 25 and 26, respectively. From Figure 25 and Figure 26 it is obvious that the numerical solutions obtained with `QUALIDAES`(rcd0) as well as `DASPK` and `ODASSL` pass the singular state independent of the used formulation. In contrast, in the numerical integration by use of `GEOMS` and `QUALIDAES` independent of the used formulation (except for `QUALIDAES`(rcd0)) the singular state is detected and the integration is stopped, which should be the correct reaction within the numerical integration process.

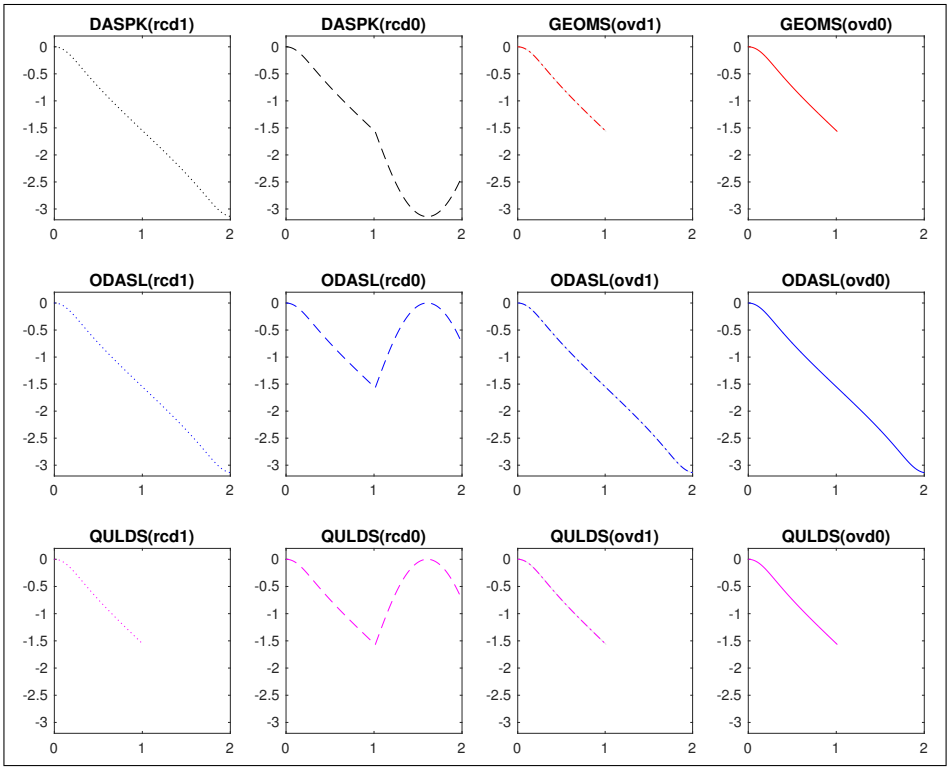

Figure 25: Scenario 04: Numerical solutions for a prescribed tolerance of RTOL=ATOL=10^{-6}

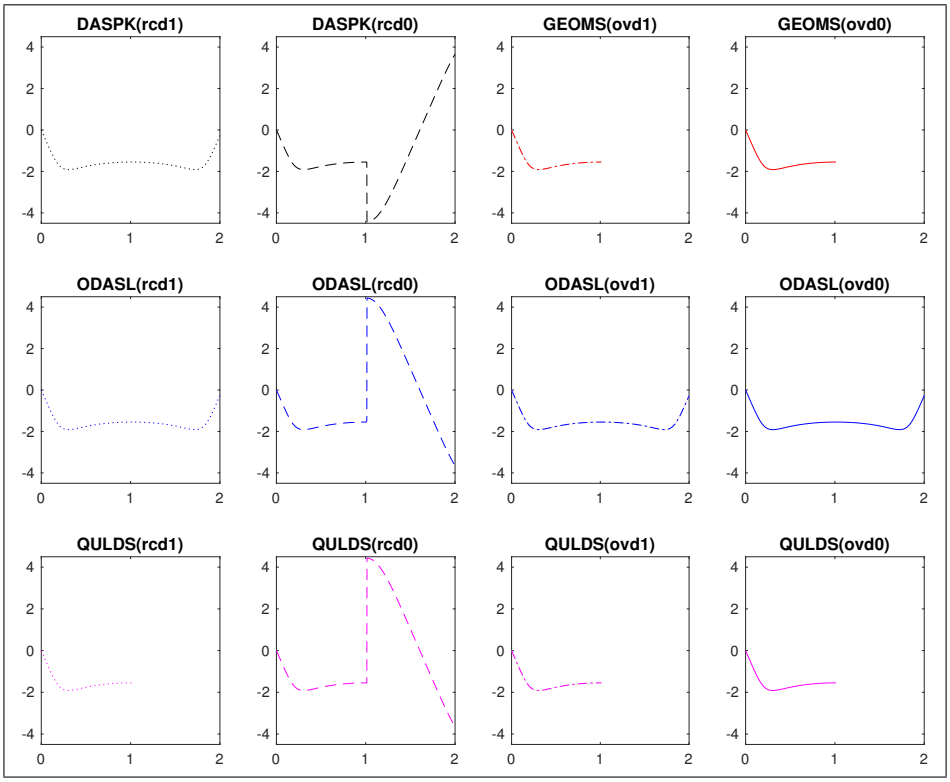

Figure 26: Scenario 04: Numerical solutions for a prescribed tolerance of RTOL=ATOL=10^{-6}

3 Summary

On the example of the *Slider Crank*, we considered the applicability, efficiency, accuracy, and robustness of different numerical solvers for differential-algebraic equations in combination with several formulations, i.e., regularized formulations or also index reduced formulations, for the model equations.

List of Figures

List of Tables

References

[1] K.E. Brenan, S.L. Campbell, and L.R. Petzold. *Numerical Solution of Initial-Value Problems in Differential Algebraic Equations*, volume 14 of *Classics in Applied Mathematics*. SIAM, Philadelphia, PA, 1996.

[2] E. Eich-Soellner and C. Führer. *Numerical Methods in Multibody Dynamics*. B.G.Teubner, Stuttgart, 1998.

[3] C. Führer. *Differential-algebraische Gleichungssysteme in mechanischen Mehrkörpersystemen - Theorie, numerische Ansätze und Anwendungen*. PhD thesis, Technische Universität München, 1988.

[4] E. Hairer, C. Lubich, and M. Roche. *The Numerical Solution of Differential-Algebraic Systems by Runge-Kutta Methods*. Springer-Verlag, Berlin, Germany, 1989.

[5] E. Hairer and G. Wanner. *Solving Ordinary Differential Equations II - Stiff and Differential-Algebraic Problems*. Springer-Verlag, Berlin, Germany, 2nd edition, 1996.

[6] P. Kunkel and V. Mehrmann. *Differential-Algebraic Equations — Analysis and Numerical Solution*. EMS Publishing House, Zürich, Switzerland, 2006.

[7] A. Steinbrecher. *Numerical Solution of Quasi-Linear Differential-Algebraic Equations and Industrial Simulation of Multibody Systems*. PhD thesis, Institute of Mathematics, Technische Universität Berlin, 2006.

[8] A. Steinbrecher. GEOMS: A new software package for the numerical simulation of multibody systems. In *10th International Conference on Computer Modeling and Simulation (EUROSIM/UKSIM 2008)*, pages 643–648. IEEE, 2008.

[9] A. Steinbrecher. M025 - spring-mass chain with path control (v1.0). Technical Report 2016/07, Institut für Mathematik, Technische Universität Berlin, Berlin, Germany, 2016.

[10] P.E. Van Keken, D.A. Yuen, and L.R. Petzold. DASPK: a new high order and adaptive time-integration technique with applications to mantle convection with strongly temperature- and pressure-dependent rheology. *Geophysical and Astrophysical Fluid Dynamics*, 80(1-2):57–74, 1995.